



POLYURETHANE/POLYETHERSULFONE DUAL-LAYER ANISOTROPIC
MEMBRANES FOR CO₂ REMOVAL FROM FLUE GAS

Christian David García Jiménez

Tese de Doutorado apresentada ao Programa de Pós-graduação em Engenharia Química, COPPE, da Universidade Federal do Rio de Janeiro, como parte dos requisitos necessários à obtenção do título de Doutor em Engenharia Química

Orientadores: Alberto Cláudio Habert
Cristiano Piacsek Borges

Rio de Janeiro
Abril de 2021

POLYURETHANE/POLYETHERSULFONE DUAL-LAYER ANISOTROPIC
MEMBRANES FOR CO₂ REMOVAL FROM FLUE GAS

Christian David García Jiménez

TESE SUBMETIDA AO CORPO DOCENTE DO INSTITUTO ALBERTO LUIZ
COIMBRA DE PÓS-GRADUAÇÃO E PESQUISA DE ENGENHARIA DA
UNIVERSIDADE FEDERAL DO RIO DE JANEIRO COMO PARTE DOS
REQUISITOS NECESSÁRIOS PARA A OBTENÇÃO DO GRAU DE DOUTOR
EM CIÊNCIAS EM ENGENHARIA QUÍMICA

Orientadores: Alberto Cláudio Habert
Cristiano Piacsek Borges

Aprovada por: Prof. Alberto Cláudio Habert
Prof. Cristiano Piacsek Borges
Prof^a. Kátia Cecília de Souza Figueiredo
Prof. Rafael Aislan Amaral
Dr. Wilson Mantovani Grava
Prof. Frederico de Araujo Kronemberger

RIO DE JANEIRO, RJ – BRASIL
ABRIL DE 2021

García Jiménez, Christian David

Polyurethane/Polyethersulfone dual-layer anisotropic membranes for CO₂ removal from flue gas / Christian David García Jiménez – Rio de Janeiro: UFRJ/COPPE, 2021.

VI, 88 p.: il.; 29,7 cm

Orientadores: Alberto Cláudio Habert
Cristiano Piacsek Borges

Tese (doutorado) – UFRJ/ COPPE/ Programa de Engenharia Química, 2021.

Referências Bibliográficas: p. 74-81

1. Preparo de membranas. 2. Captura de CO₂. I. Habert, Alberto Cláudio *et al.* II. Universidade Federal do Rio de Janeiro, COPPE, Programa de Engenharia Química. III. Título.

Resumo da Tese apresentada à COPPE/UFRJ como parte dos requisitos necessários para a obtenção do grau de Doutor em Ciências (D.Sc.)

MEMBRANAS ANISOTRÓPICAS DE DUPLA CAMADA DE
POLIURETANO/POLI(ÉTER SULFONA) PARA CAPTURA DE CO₂ DO GÁS
DE COMBUSTÃO

Christian David García Jiménez

Abril/2021

Orientadores: Alberto Cláudio Habert

Cristiano Piacsek Borges

Programa: Engenharia Química

Este trabalho estuda o preparo de membrana de poliuretano / poli(éter sulfona) de camada dupla pela técnica de co-casting. Os efeitos do tempo de evaporação e da temperatura do banho de água de coagulação na morfologia da membrana são avaliados. Camadas uniformes com excelente adesão são obtidas. Membranas de dupla camada de matriz mista são preparadas com duas partículas diferentes: carvão ativado e sílica. Os efeitos do teor de partícula na morfologia da membrana são explorados. A adesão e a estrutura homogênea das camadas são mantidas para teores baixos de partícula. Para membranas sem partículas, aumentar a pressão de 1 a 8 bar resulta em uma redução da permeabilidade de CO₂ e seletividade ideal de CO₂/N₂ de 19,6 para 13,0 Barrer e de 66 para 60, respectivamente. Temperatura na faixa de 25 a 45 °C aumenta a permeabilidade ao CO₂ de 19,6 a 28,9 Barrer, embora a seletividade do CO₂/N₂ diminua de 66 para 43. No caso das membranas de matriz mista, a presença de carvão ativado e sílica aumenta a permeabilidade ao CO₂ de 19,6 para 22,6 e 23,1 de Barrer, respectivamente. Além disso, valores mais elevados de pressão de alimentação levam a um aumento de mais de 40% na permeabilidade ao CO₂ para as membranas com carvão ativado, apresentando bom potencial para tratamento de gases de combustão.

Abstract of Thesis presented to COPPE/UFRJ as a partial fulfillment of the requirements for the degree of Doctor of Science (D.Sc.)

POLYURETHANE/POLYETHERSULFONE DUAL-LAYER ANISOTROPIC
MEMBRANES FOR CO₂ REMOVAL FROM FLUE GAS

Christian David García Jiménez

April/2021

Advisors: Alberto Cláudio Habert
Cristiano Piacsek Borges

Department: Chemical Engineering

This work studies the preparation of dual-layer polyurethane/polyethersulfone membranes using the co-casting technique and the effects of the evaporation time and the temperature of the coagulation water bath on the membrane morphology are evaluated. Uniform layers with excellent adhesion are obtained. Also, the preparation of dual-layer mixed matrix membranes is carried out with two different particles: activated carbon and silica. The effects of particle content on membrane morphology are explored. The adhesion and homogeneous structure of the layers are maintained at low particle content. For non-particle membranes, increasing the pressure from 1 to 8 bar results in a reduction of CO₂ permeability and CO₂/N₂ ideal selectivity from 19.6 to 13.0 Barrer, and from 66 to 60, respectively. Temperature in the range of 25 to 45 °C enhances CO₂ permeability from 19.6 to 28.9 Barrer, although CO₂/N₂ selectivity decreases from 66 to 43. In the case of mixed matrix membranes, the presence of activated carbon and silica enhances CO₂ permeability from 19.6 to 22.6 and 23.1 Barrer, respectively. Moreover, higher feed pressure values lead to an increase of more than 40% in CO₂ permeability for the membranes with activated carbon, showing good potential for flue gas treatment.

Content

1. Introduction	1
1.1. Objectives.....	4
1.1.1. Specific Objectives	5
1.2. Structure of this thesis	5
2. Fundamentals and state-of-art	7
2.1. Membrane processes.....	7
2.2. Gas transport through membranes	9
2.3. Polymers used for gas permeation processes.....	14
2.3.1. Polyurethane.....	14
2.4. Membrane Preparation Methods	15
2.4.1. Sintering.....	15
2.4.2. Stretching.....	15
2.4.3. Track-etching	15
2.4.4. Melting polymer extrusion	16
2.4.5. Phase inversion	16
2.5. Phase inversion method.....	17
2.5.1. Solvent evaporation.....	18
2.5.2. Controlled evaporation.....	18
2.5.3. Vapor presence	18
2.5.4. Immersion	19
2.6. Non-solvent induced phase inversion by immersion.....	19
2.6.1. Thermodynamics in immersion method.....	22
2.6.2. Influence of some variables on membrane morphology.....	25
2.7. Dual-layer membranes.....	28
2.8. Mixed Matrix Membranes	32
2.9. State of the art and this research proposal.....	34
3. Polyurethane/Polyethersulfone dual-layer anisotropic membranes for CO ₂ removal from flue gas	35
4. Polyurethane/Polyethersulfone mixed matrix dual-layer membranes containing inorganic particles for CO ₂ removal from flue gas	52
5. MAIN CONCLUSSIONS AND FINAL COMMENTS.....	70
REFERENCES.....	74
ANNEX: DETAILED METHODOLOGY OF MEMBRANE SYNTHESIS AND CHARACTERIZATION.....	82

1. Introduction

Flue gas is one of the major wastes resulting from the burning of fuels and other kind of processes in the industry. Table 1 shows some of the main gases contained in flue gas and some of the standard conditions. It contains, among other contaminant gases, carbon dioxide (CO₂), the major greenhouse gas that has effect in the climate change (Zhao et al., 2016).

TABLE 1.1. TYPICAL PROPERTIES OF COAL-FIRED FLUE GAS AFTER SO₂ SCRUBBING IN POST-COMBUSTION CARBON CAPTURE (ZHAO ET AL., 2016).

Flue gas	Composition or condition	Kinetic diameter (Å)
CO ₂	10–16 wt%	3.30
N ₂	70–75 wt%	3.64
H ₂ O (vapor)	5–7 wt%	2.65
O ₂	3–4 wt%	3.45
CO	~20 ppm	3.75
NO _x	< 400 ppm	
SO _x	< 400 ppm	
Temperature	45–120 °C	
Pressure	~ 1 bar	

As it can be seen, it contains a high amount of carbon dioxide (CO₂), the major greenhouse gas that has effect on climate change. CO₂ emissions during the last decades are shown in Figure 1.1.

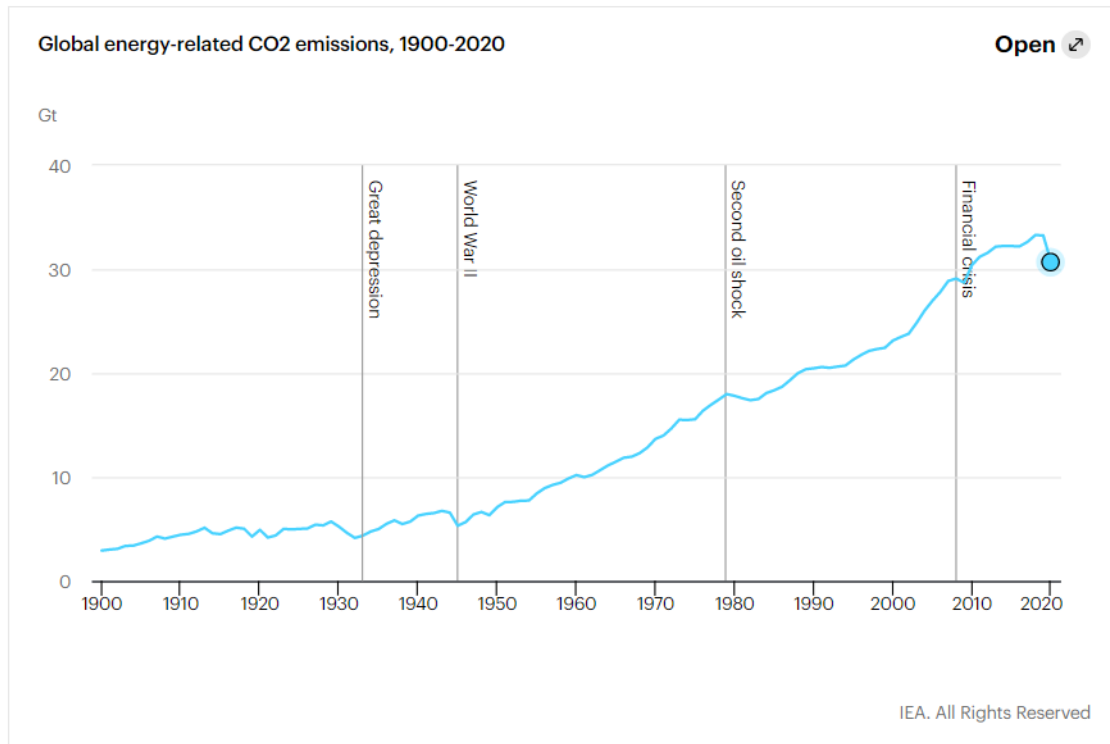


Figure 1.1. CO₂ emissions during the last decade. Source: International Energy Agency (IEA)

The figure shows that CO₂ emissions have been increasing during the last decades reaching about 30 Gt in 2020, about 6 times higher than 70 years ago. Therefore, CO₂ capture has become of great importance to reduce global warming. Post-combustion capture is the name given to the process where CO₂ is removed from the flue gas (Arias et al., 2016; Khalilpour et al., 2015). Currently, there are three widely studied technologies for carbon capture: pre-combustion capture, post-combustion capture (PCC) and oxy-fuel combustion. However, post-combustion carbon capture still has challenges to overcome mainly due to the typical properties of flue gas: low pressure (~ 1 bar), high temperature (45 ~120 °C), low concentration of CO₂ (<16 wt%) and almost no difference in the molecular size of the main gases.

Membrane processes are one of the most recent alternatives for CO₂ capture. The main advantages against other technologies include compactness, modularity, ease of installation by skid-mounting, ability to be applied in remote areas (such as offshore), flexibility in operation and maintenance, and, in most cases, lower capital cost as well as lower energy consumption (Abanades et al., 2015; J. L. Li & Chen, 2005; Thorbjörnsson et al., 2015; Xia et al., 2018a; Zhao et al., 2016).

Membrane research and development for CO₂ capture could be divided into two categories: membrane material design (MMD) and membrane systems engineering (MSE). The fundamental goal of MMD is to synthesize membranes of desirable permeance and selectivity while having chemically and physically stable structures. On the other hand, the major goal of MSE is to develop membrane capture processes with optimal configurations to achieve the separation targets (Dai et al., 2016; Khalilpour et al., 2015).

In the field of MMD for dense membranes (more commonly used for gas separation), the major advantage of them is that there is a high tunable degree of controlling the membrane permeability and selectivity via the manipulation of polymer preparation and chemical composition. Counteracting this are: the high mass transfer resistance due to the membrane thickness, and characteristic swelling and plasticization of the materials as a result of CO₂ absorptions.

Dual-layer membranes are an interesting alternative to try overcome the limitations of the dense membranes. These membranes are formed by at least two layers: a selective layer for species separation and a support (non-selective) layer to achieve mechanical properties requirements. This membrane

morphology allows the use of different material in each layer, making possible to combine both high permeability and selectivity, and at the same time to save materials used in the selective layer. There are several methods to prepare dual-layer membranes, among them, the co-casting of two solutions, which reduce the preparation time and allows the use of solvents that can dissolve both polymers used in the fabrication process (Hashemifard et al., 2011a; Karimi & Hassanajili, 2017a; X. M. Li et al., 2010a). However, the adhesion of layers of different materials plays an important role in dual-layer membrane preparation (X. M. Li et al., 2010a; Naderi et al., 2019; Ullah Khan et al., 2018a; Xia et al., 2018b)

On the other side, it is possible to incorporate inorganic nanoparticles into the selective layer to increase its performance by incorporating nanoparticles into it. These membranes are called mixed matrix membranes (MMMs) and combine the advantages and versatility of the polymeric membranes with the separation properties of the inorganic materials. The inorganic fillers can be solid (impermeable) or porous (permeable). Activated carbon is a versatile porous filler used for CO₂ capture because of its high surface area and pore size distribution. On the other hand, the use of silica as a solid filler has resulted into an enhancement of membrane permeability in CO₂ capture processes.

1.1. Objectives

The main objective of this research is to prepare dual-layer membranes for CO₂ removal from flue gas, specifically from N₂ and O₂.

1.1.1. Specific Objectives

- To study the effect of the synthesis conditions during preparation process on membrane morphology
- To find the best conditions to prepare efficient dual-layer membranes by the immersion – precipitation method.
- To study the effect of pressure and temperature on the performance of dual – layer membranes.
- To incorporate nanoparticles into dual-layer membranes in order to improve selectivity and permeability.
- To determine the effect of particle nature and content on membrane morphology and performance.

1.2. Structure of this thesis.

As it was showed in the previous section, the aim of this thesis is to study the preparation of dual-layer membranes. Since the main results were object of two submitted publications in peer reviewed scientific journals, and for the sake of objectiveness, the article format were kept as separate chapters 3 and 4.. However, additional comments were included in each chapter in order to provide a more detailed discussion of the results. According to this, the Thesis structure is:

- Section 2: Fundamentals and State of Art. The main focus of this section is to show previous works related to dual-layer membrane preparation,

specifically those related to the co-casting technique. The advantages of this process are also showed.

- Section 3 (Article I): *Polyurethane/Polyethersulfone dual-layer anisotropic membranes for CO₂ removal from flue gas*. Journal of Applied Polymer Science. Published on January 2021 (<https://doi.org/10.1002/app.50476>).
- Section 4 (Article II): *Polyurethane/Polyethersulfone mixed matrix dual-layer membranes containing inorganic particles for CO₂ removal from flue gas*. Journal of Applied Polymer Science. Under revision, submitted February 2021.
- Section 5: Main conclusions and advances in the state-of-art. Also, some suggestions for future works are given.

Moreover, considering that in article format the experimental procedures have to be concise, further details for the methodology section are given in the annex section.

This work was undertaken in the Membrane Separation Processes Lab. of COPPE/UFRJ, where substantial previous progress on membrane synthesis and applications were obtained in recent years. Also, CAPES and CNPq (Ref. 141762) provided a scholarship to support the development of this thesis.

2. Fundamentals and state-of-art

2.1. Membrane processes

In general, a membrane can be defined as a barrier which separates two phases so it can totally or partially restrict the transport of one or various chemical species present in the phases

In membrane separation processes, the fluid that permeates through the membrane is called permeate and the fraction of the process feed that is retained is called retentate, as it is shown in Figure 2.1. Under the action of a driving force, separation is achieved due to the membrane's properties to selectively transport one of the components of the feed.

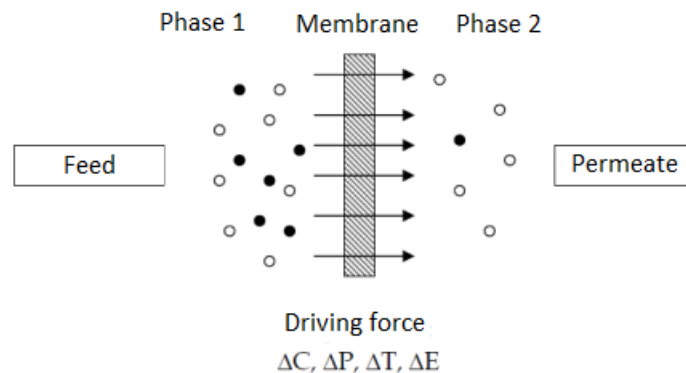


Figure 2.1. Membrane process (adapted from MULDER, 2000).

The separation processes through membranes can be classified according to the driving force used to promote permeation. Reverse osmosis, ultrafiltration, microfiltration and nanofiltration use the difference in pressure between the feed and the permeate as the driving force of. Dialysis uses the concentration gradient, pervaporation and gas separation use the difference in partial pressure between

the feed and the permeate of the component of interest; and the electro dialysis presents the electric potential difference as a driving force.

Membranes can also be classified as dense or porous; or, according to their morphology, as isotropic or anisotropic, as it is shown in Figure 2.2.

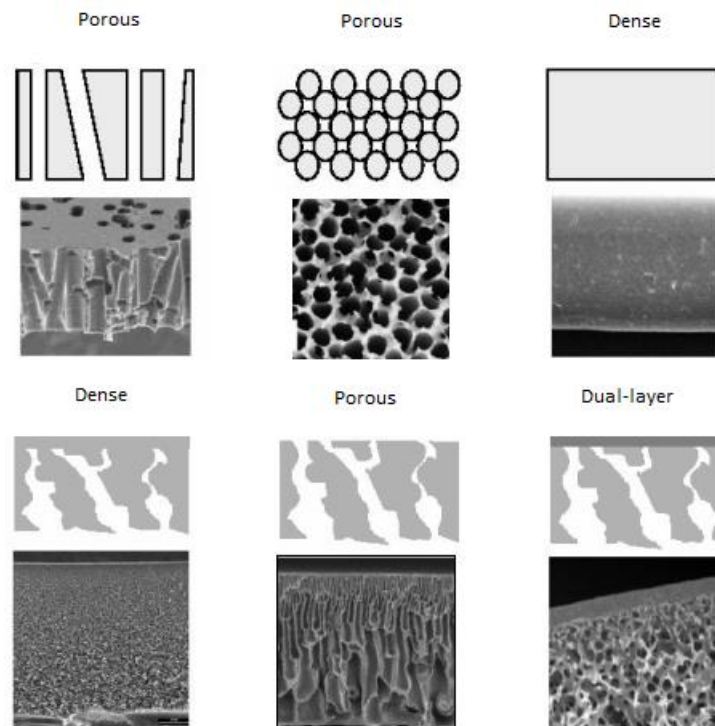


Figure 2.2. Membrane morphologies (adapted from HABERT *et al.*, 2006).

Isotropic membranes have the same morphology across the cross section. Anisotropic membranes have a very thin upper region ($1\mu\text{m}$), more impermeable (porous or not), called skin, which it is supported by a porous (more permeable) structure. When both regions are made of a single material, the membrane is called integrated anisotropic and when they are of different materials, it is called anisotropic dual-layer.

In gas separation processes by polymeric membranes, both dense and porous membranes are used. In this second case, the sizes of pores are on the order of 5 to 20 Å, so gases can be separated by size, by molecular sieve mechanisms; or by Knudsen diffusion, in which the membranes pores (<0.1µm) have an equivalent diameter smaller than the average free path of the gas molecule. In membranes with larger pores (from 0.1 to 10µm), the permeate gas flow is convective and there is no gas separation. Although the use porous membranes is of great interest in various applications, most of the industrial gas separation plants use dense membranes. The most accepted theory for membrane gas separation accepted to describe the transport of gases through dense polymeric membranes is the classic sorption-diffusion mechanism (BAKER, 2004).

2.2. Gas transport through membranes

Figure 2.3 shows two main kind of membranes used in gas separation: porous and dense membranes. In porous membranes, depending on the pore size, the gas is separated by molecule size difference and the mechanism that predominates is Knudsen's diffusion. The most used membranes for gas permeation are dense membranes in which the selectivity depends on the affinity of the different species with the membrane material, with a thermodynamic step (sorption of the molecule into the polymer matrix) and a kinetic step (diffusion of the molecule through the polymer). So, in these membranes, the key stage for a high permeate flow is the diffusive one regardless of the type of driving force

applied, since the membrane does not have pores close to the surface that is in contact with the gas mixture.

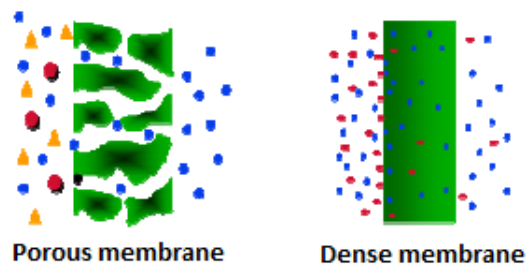


Fig 2.3. Gas permeation through porous and dense membranes adapted from HABERT *et al.*, 2006).

For dense membranes, the main variables involved in these steps are temperature, pressure, concentration, molar mass, molecule size and shape, polymer/molecule compatibility, crosslinking and crystallinity of the polymeric material (HABERT *et al.*, 2006).

The mechanism used to describe gas transport in dense membranes is sorption-diffusion and the steps are showed in Figure 2.4; where c_1 is the concentration of the component of interest, μ_1 is the chemical potential of the component of interest, and I , m and II represent the feed side, membrane and permeate side, respectively.

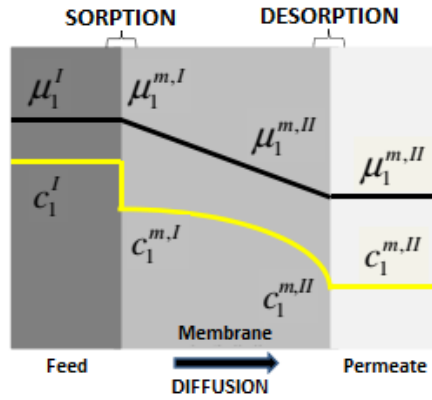


Fig 2.4. Transport through dense membranes (adapted from Silva, 2016).

The transport is caused by the action of a driving force (chemical potential) such as the pressure difference between both sides of the membrane which is selective to one of the components. First there is a diffusion of gases on feed side (side with the highest partial pressure) through the boundary layer generated by the selectivity of the membrane (1); then, gas molecules dissolve through the polymer (2); gas molecules diffuse through the polymeric matrix, from the highest to the lowest gas partial pressure (3). After that, gas desorption occurs on the permeate side (4); and finally, the diffusion through the boundary layer on the permeate side happens (5). It should be noted that, for gas transport, there are several cases where the boundary layers both on the feed and on the permeate side (steps 1 and 5) generally represent small influence and resistance and they can be neglected (CRANK & PARK, 1968).

The total flux through the membrane for a component i can be calculated using:

$$J_i = -D_i \frac{dc_i}{dx} \quad (2.1)$$

where J_i is the flux of the component i , D_i is the diffusion coefficient for the component in the polymer matrix and dc_i/dx is the concentration (chemical potential) for i . This equation can be written in terms of the Fick Law:

$$J_i = \frac{D_i(c_{i0(m)} - c_{i(m)})}{l} \quad (2.2)$$

where l is the membrane thickness, and $c_{i0(m)}$ and $c_{i(m)}$ are the molar concentrations for i in the interphase feed – membrane and in the membrane, respectively. Also, the concentration of component i that solubilizes into the polymer matrix close to the interface with the feed is:

$$c_{i(m)} = S_i p_i \quad (2.3)$$

where p_i is the partial pressure for the component i in the interface feed – membrane and S_i is the sorption coefficient for the component i . So, the Fick equation can be written as:

$$J_i = \frac{D_i S_i (p_{i0} - p_{i1})}{l} \quad (2.4)$$

The product $D_i S_i$ is known as the permeability P_i , for the component i in the membrane leading to the equation:

$$J_i = \frac{P_i (p_{i0} - p_{i1})}{l} \quad (2.5)$$

This equation is widely used to describe gas permeation in membranes. However, it is restricted to systems that behave according to these considerations:

- Transport is caused mainly by the concentration gradient in the membrane

- The dissolution of a component within the membrane is linearly proportional to its activity in the adjacent gas.

In glassy polymers, where the diffusion stage limits the transport, the permeability is drastically reduced when penetrant molar mass increases. On the other hand, in elastomeric polymers, p_{isat} (saturation pressure of component i) can be the dominant term and permeability increases with molar mass up to a certain limit value (BAKER and WIJMANS, 1995).

So, permeability can be calculated from the permeate flux through the membrane, using the values of the membrane thickness l and the partial pressure through the membrane. The most common units for gas permeability are Barrer, with 1 Barrer being equal to $10^{-10} \text{ cm}^3(\text{CNTP}).\text{cm}/(\text{cm}^2.\text{s}.\text{cmHg})$ or GPU (Gas Permeation Unit) used for porous and dual – layer membranes, being a measure of gas permeability by unit of membrane thickness (P/l), with 1 GPU equal to $10^6 \text{ cm}^3(\text{CNTP})/(\text{cm}^2.\text{s}.\text{cmHg})$.

The membrane efficiency is also dependent on a separation factor α_{AB} (assuming a binary mixture), called selectivity. This can be calculated by:

$$\alpha_{AB} = \frac{y_a/y_b}{x_a/x_b} \quad (2.6)$$

where A and B are two components of the mixture, y_i and x_i are the concentration of i in the permeate and feed side, respectively. Assuming that the pressure on the permeate side is much lower than in the feed side and that the gases have low interaction between them, the separation factor can be reduced to an ideal selectivity α_{AB}^* . It can be defined as a ratio between the permeability for the pure components or between both their sorption and diffusion coefficients.

$$\alpha_{AB}^* = \frac{P_A}{P_B} = \frac{D_A S_A}{D_B S_B} \quad (2.7)$$

Some of the factors that mostly affect the diffusivity are: segmental mobility for the polymer chains, attraction between chains, permeant size, gas composition, free volume in the polymer matrix and temperature. On the other side, the solubility depends mainly on the gas condensability into the polymer and also on the polymer – permeant interactions. Then, it is important to discuss the effects of sorption and diffusion on membrane performance.

2.3. Polymers used for gas permeation processes

2.3.1. Polyurethane

Polyurethane is a polymer that has the urethane functionality, with a segmented structure, originated by the polycondensation reaction of an isocyanate (bi or polyfunctional), responsible for the rigidity of the material, and a polyol, responsible for flexibility, in addition to other reagents, such as curing agents or extenders chain, and can be rigid or flexible. Isocyanates can be aromatic or aliphatic. Polyols can be polyethers or polyesters, while chain may be water, glycol, polyol, diamine or amyl alcohols. The most common polyols used in the manufacture of PU's are the polyether polyols followed by the polyols polyesters. As for isocyanates, the most used are based on toluene diisocyanate (TDI) and methylene diphenyl isocyanate (MDI) and its derivatives, which are obtained from diamines.

Elastomeric polymers, such as polyurethane, have two characteristics main structural elements: high flexibility of the polymer chains (that is, they have glass transition temperature below room temperature) and chemical or physical

cross-links. The flexibility of the chains allows high deformation, while the cross links prevent the chain from slipping, thus producing a plastic deformation.

2.4. Membrane Preparation Methods

2.4.1. Sintering

In this method, the polymer in powder form is pressed and sintered at high temperature, giving result to microporous membranes with pore size greater than 1 μm . Poly (ethylene), poly (tetra-fluorethylene) and poly (propylene) are some examples of polymers that can be used in this technique. Inorganic materials can also be employed. (Van't Hoff, 1988; Mulder, 1991; Baker 2004).

2.4.2. Stretching

In this process, a dense polymeric film is deformed perpendicular to the direction of extrusion, so that there are small breaks in the material, resulting in membranes with pore size in the order of 0.1 to 3 μm . In this technique, only semi-crystalline polymers, such as poly (ethylene) and poly (propylene), can be used.

2.4.3. Track-etching

In this technique, a dense polymeric film, usually of poly (carbonate), is exposed to radiation. After this stage, a washing with caustic solution follows, which promotes the erosion of bombed spots. Radiation weakens polymer chain

links, forming trails. Weakened sites are attacked by the solution, letting to cylindrical and uniform pores, with narrow size distribution. The achieved porosity is low and depends on the exposure time of the film to radiation. The pore size is controlled through the contact time of the film with the solution, reaching the range of 0.02-10 μm .

2.4.4. Melting polymer extrusion

Dense isotropic membranes, flat or in the form of hollow fibers, can be produced by cooling a molten polymer (Van't Hof, 1988). Membranes with such morphology have very low permeability, which would not be advantageous from an industrial point of view. However, these membranes are normally used for characterization of the intrinsic transport properties in polymeric materials for gas separation. This method for membrane preparation can also be used in the case of polymers that are not easily dissolved in environment conditions.

2.4.5. Phase inversion

By this technique, a polymeric solution is spread as a thin film or extruded like a hollow fiber. The membrane results from phase separation when the polymer solution equilibria is affected by a change in temperature or solubility. Most polymeric membranes available on the market, including OI and NF, are obtained through the phase inversion technique. Because of this, this technique will be more discussed in the next section.

2.5. Phase inversion method

The phase inversion process is characterized by the destabilization of a solution polymeric, obtained by inducing the state of supersaturation, promoted by changes in its chemical nature, composition, temperature or pressure. In this way, the solution becomes intrinsically unstable or metastable and tends to separate into at least two liquid phases of different compositions. In membrane preparation, the rich phase will form the polymer matrix structure and the other phase, poor in polymer, will lead to the pores (Kesting, 1985; Baker et al., 1991; Mulder, 1991; Nunes and Peinemann, 2001; Baker, 2004). With the progress of the phase separation process, increasing the concentration of polymer in the rich phase will increase its viscosity, making it difficult to transfer mass in the system. Often, these viscous effects can difficult the achievement of the thermodynamic balance between the phases, leading to the solidification of the structure and formation of the membrane. This solidification process is linked to phenomena such as crystallization, gelation and / or vitrification, and depends on the physicochemical nature of the polymer-solvent system (Kesting, 1985; Mulder, 1991; Baker, 2004).

There are different methods to cause this phase inversion: chemical reaction, thermal-induced and composition variation, being the last one commonly used for anisotropic membrane preparation. In this method, precipitation occurs due to changes in the composition of the polymeric solution, caused by the mass transfer between two phases in contact. This is the most used technique in membrane preparation and the precipitation of the solution can be done in different ways:

2.5.1. Solvent evaporation

A polymeric solution containing only one polymer and a suitable solvent is spread on a support, for example, a glass plate, and exposed to an inert nitrogen atmosphere (to avoid interference from water vapor present in the atmosphere). The fixation of the polymeric matrix occurs by evaporation of the solvent, which favors viscous effects due to the gradual increase in polymer concentration, normally originating dense isotropic membranes (Mulder, 1991; Baker, 2004).

2.5.2. Controlled evaporation

In this technique, a polymer is dissolved in a mixture of a volatile solvent and a less volatile non-solvent. The resulting solution is exposed to the environment. Solvent evaporation causes an increase of the polymer concentration in the solution until precipitation occurs, due to the presence of the non-solvent. The relative rate of evaporation may allow the formation of anisotropic membranes with dense skin (Mulder, 1991; Baker, 2004).

2.5.3. Vapor presence

In this case, a polymeric film composed only of polymer and solvent is exposed to an atmosphere containing vapors from the solvent itself and a non-solvent, so solvent evaporation is affected and liquid-liquid phase separation occurs when the non-solvent enters the solution. Since precipitation occurs in polymeric concentrations lower than the initial one, it is possible to obtain isotropic porous membranes (Mulder, 1991; Baker, 2004).

2.5.4. Immersion

This technique consists of immersing a polymeric film, flat (Fig 2.5) or in the form of fiber hollow, in a non-solvent bath. In this method, the transport of components between the two phases in contact, solvent for the bath and non-solvent for the film will cause the liquid-liquid phase separation and subsequent precipitation of the polymeric solution (Mulder, 1991; Baker, 2004). In some cases, before immersion in the precipitation bath, there may be an intermediate stage in which the polymeric film is exposed to ambient air for partial evaporation of the volatile solvent. The immersion technique is used in the preparation of membranes for all types of separation processes. Because of this, this method will be discussed with more details in the next section.

2.6. Non-solvent induced phase inversion by immersion

Taking into account the large number of variables and materials involved, precipitation by immersion is the one that enables greater flexibility and, consequently, a wide variety of morphologies for the produced membranes. In addition, important characteristics of membranes, such as thickness and porosity of dense skin and porosity of the porous support can be, in a way, controlled in the immersion-precipitation process, allowing the obtention of suitable membranes for a given application, including for RO and for NF.

The first report on the synthesis of membranes by the immersion method is dated 1872 and was made by Baranetzky, aiming at the preparation of flat nitrocellulose membranes (Pierce, 1927). Only in the following century, in 1963,

the first commercially accepted membranes were achieved. The researchers Loeb and Sourirajan (1962) developed anisotropic osmosis membranes for water desalination combining high selectivity and permeability, consolidating the membrane synthesis technology.

The permanent challenge is simply to improve the performance of membranes existing or obtain a highly selective membrane with the lowest layer thickness (skin) possible, free from defects and that at the same time can be resistant both mechanically and chemically. The most used techniques to obtain these membranes are casting and extruding. In simple casting, one polymeric solution is placed on a plate and immersed in a non-solvent bath (Pitol-Filho et al. 2006).

When preparing a flat polymeric membrane, the solution is placed on an appropriate support and processed using a spreading knife with specific thickness. In laboratory, the most commonly used supports are glass, metal or plastic plates. In industrial scale, it is used non-woven paper as support material for the membranes.

After spreading, the polymeric film can be exposed to the environment for certain period. This preliminary stage is used as an important factor for the formation of the skin layer and will depend on the solvent volatility. The preferential evaporation of a volatile solvent will increase the concentration of the polymer in the surface of the solution, consequently causing a more asymmetric polymer on the top. In this way, the thickness and / or density of the skin will be a function of the exposure time of the polymeric solution. On the other hand, the absorption of water vapor from ambient air (Figure 2.5 (a)) will be predominant if

the solvent volatility is small, since there will be a closer approximation of the more superficial layers of liquid-liquid phase separation, which can lead to formation of porous membranes.

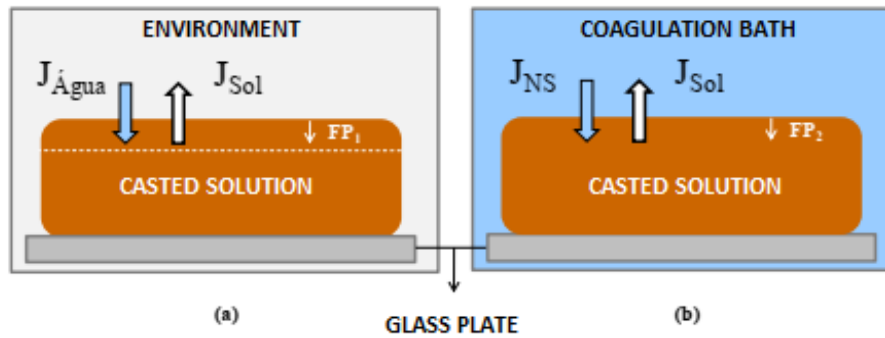


Figure 2.5. Casting process (a) during exposition to environment, (b) after immersion into the coagulation bath.

In the next step, the polymeric film is immersed in a coagulation bath consisting of a non-solvent for the polymer or a solvent / non-solvent mixture. Due to the difference in chemical potential of the solvent and the non-solvent between the two phases in contact, as represented in Figure 2.5 (b), will be a solvent flow into the bath and a non-solvent flow into of the polymeric solution. This exchange of components has two immediate consequences: the interface between the film and the bath is mobile and the composition of the film is a function of time and position.

Usually, the solvent flow is greater than the non-solvent flow, causing a gradual increase in polymer concentration at the film / bath interface and consequent increase in resistance to mass transfer. This increase in polymer concentration can lead to conditions where the viscous effects prevent that liquid-liquid phase separation is achieved, so the membrane, in this case, is formed by solidification phenomena, such as gelation, crystallization and / or vitrification. On

the other hand, depending on the conditions involved in the transport of mass, the presence of non-solvent in the polymeric film can promote an immediate liquid-liquid phase separation, initiated in the interfacial layers and propagated towards the support. The dissolved polymer phase, which leads to the pores, can grow until the increasing in polymer concentration leads to solidification of the rich phase, creating the membrane structure across the casted film (Carvalho, 2005).

Finally, the membrane may be washed with non-solvent to remove residual solvent and then dried. Water is the most common non-solvent used in synthesis of commercial membranes due to its low cost compared to others and the ease of obtaining.

2.6.1. Thermodynamics in immersion method

The description of the system in terms of the compositions that determine regions of stability and instability for the polymeric solution can be done based on the variation of the free energy of mixing (ΔG_M) and the concentration of the polymer in the solution polymeric (Bulte et al., 1996).

For a generic system with N components, the free energy of mixing ΔG_M can be expressed as:

$$\Delta G_M = \Delta H_M - T\Delta S_M \quad (2.8)$$

where ΔH_M is the enthalpy of mixing, T is temperature and ΔS_M is the entropy of mixing. In polymeric solution systems the contribution of the enthalpic term is the thermodynamic factor that determinates the miscibility of the system.

Phase separation will occur when a state thermodynamically unstable is reached, due to disturbances in temperature (T), pressure (P) or composition of the solution, in order to minimize the free energy of mixing. In this case, it can only be said that, at specified T and P, the mixture is more stable than the pure components. The criteria for minimizing free energy and for local thermodynamic stability are given, respectively, by:

$$(\Delta G_M)_{two\ phases} < (\Delta G_M)_{one\ phase} \quad (2.9)$$

$$\left[\frac{\partial^2(\Delta G_M)}{\partial^2 n_i^2} \right]_{T,P,n_{j \neq i}} > 0 \quad (2.10)$$

If the stability criterion is not met, the system will be divided into two or more phases. From this statement, the systems can be classified as having total miscibility, partial miscibility and total immiscibility. For a generic system which presents partial miscibility, the schematic representations of the energy free of mixing and its second derivative as a function of the polymer volume fraction are shown in Figure 2.6.

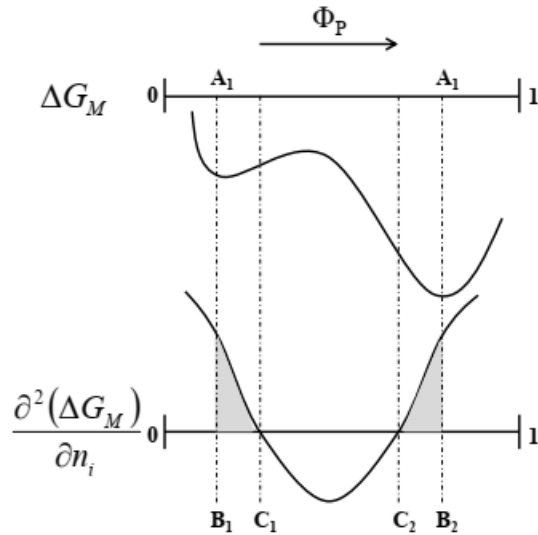


Figure 2.6. Upper: Representation of the variation in free energy of mixing as a function of polymer concentration ϕ , Lower: Representation of the second derivative curve for the free energy of mixing for the composition of the polymeric solution. Source: Carvalho (2005).

In the previous figure, three distinct regions can be distinguished depending on thermodynamic stability conditions: stable, metastable and unstable region. The points A, B and C delimit regions with different characteristics and represent the minimum, tangent and inflection points, respectively. The compositions in the region between points C1 and C2 do not meet the stability criterion (the second derivative is lower than zero), so they are thermodynamically unstable. The compositions located in the regions between B1-C1 and C2-B2, although satisfying the criterion of local stability, present favorable conditions for liquid-liquid phase separation and are called metastable. Solutions whose polymer compositions are between 0 and B1 and between B2 and 1, satisfy all conditions of stability, this region being considered stable.

2.6.2. Influence of some variables on membrane morphology

2.6.2.1. Exposure time

As it is mentioned in a previous section, during the membrane preparation process by immersion, an additional stage where the film is exposed to the environment (prior to immersion) can be performed. Depending on the characteristics and volatility of the solvent in the polymeric solution, there can be two different situations:

2.6.2.2. Polymeric solution containing a volatile solvent

In this case, the solvent flux (J_{Sol}) leaving the polymer phase (during the exposure time) will be decisive over the non-solvent inlet flow (J_{NS}) in the same phase (during precipitation). Thus, the greater the time the solution is exposed to the environment, the greater the amount of solvent volatile that will be evaporated, delaying the liquid-liquid phase separation and increasing the polymer concentration at the film / environment interface, which, consequently, brings the solution closer to the region where the viscous effects occur. In this sense, the evaporation of the solvent promotes an asymmetric distribution in the polymer concentration across the cast film, and it can form a dense surface layer, even before the solution is immersed in the precipitation bath. So, if the polymeric film remains exposed to the environment, the obtained membranes can be dense, and useful for gas separation processes.

2.6.2.3. Polymeric solution containing a non-volatile solvent

Unlike the previous case, the non-solvent inlet flow (J_{NS}) in the polymeric phase (during precipitation) is more considerable than the flow (J_{Sol}) that leaves this phase towards the air atmospheric (during exposure time). Thus, there may be the absorption of the non-solvent by the polymeric solution, so that precipitation is possible at the film / atmospheric air interface. Depending on the contact time of the polymer solution with the environment, this front of precipitation may advance significantly before the immersion of the film in the coagulating bath. Normally, in these precipitation conditions, membranes are obtained anisotropic with porous skin or porous membranes typical of those used in processes like Microfiltration and Ultrafiltration.

2.6.2.4. Coagulation bath composition

Initially, the increase in the amount of solvent in the coagulation bath, besides causing a drop in the non-solvent activity in the bath phase, also causes a decrease in the chemical potential gradient between the two phases present in the process. These facts will consequently result in a lower non-solvent flow (J_{NS}) from the bath to the polymeric solution and a lower solvent flow (J_{Sol}) of the solution for the precipitation bath. In this way, the addition of solvent promotes a decrease in the initial mass transfer rates between the phases, acting on the to delay liquid-liquid separation. In these conditions, the delay in precipitation of the solution favors the reduction of the pore size in the region close to the interface.

On the other hand, the presence of solvent in the precipitation bath can also cause the formation of membranes with larger surface pores. When the polymeric film is immersed in the precipitation bath, the solution near the interface is in equilibrium with this, forming a pair of compositions given by a mooring line. In this case, the composition of the film surface is represented by the concentrated phase composition polymer, while the diluted phase indicates the composition of the precipitation. If the solvent concentration in the bath is higher, the composition of balance on the film surface is more diluted in polymer, which, consequently, favors the process of nucleation and growth.

2.6.2.5. Effect of polymeric solution composition

Another parameter that influences the final properties of the membranes is the concentration of polymer in the solution used in the synthesis process. Increased concentration of the polymer in the casted film promotes an increase in its concentration in the film / coagulation bath interface. This fact, in addition to causing greater resistance to diffusive solvent and non-solvent transport between phases involved in the process, can also delay liquid-liquid separation in the layers of the polymeric phase, bringing them closer to the region where the viscous effects appear. In these conditions of precipitation, it is possible to obtain anisotropic membranes with dense and thick surface skins.

2.7. Dual-layer membranes

Historically, the invention of the first dual-layer anisotropic membrane was made in 1979 by Henne et al. These authors studied the production of hollow fibers cellulose base regenerated in both layers and with particles of an absorbent material in the skin layer to be tested in dialysis processes (Henne et al., 1979; Henne et al., 1981).

In another work, Groebe et al. (1987) investigated the preparation of integral flat membranes by immersion-precipitation. The polymers used were poly (acrylonitrile), cellulose acetate and poly (urethane). The analysis of the obtained flat membrane morphology showed that there was a delamination (separation) between the layers formed from each solution. However, the authors did not have any discussion about the reasons that promoted such delamination. Also in 1987, Yanagimoto developed flat and hollow fiber dual-layer hollow fibers with greater resistance to be applied in UF and MF processes (Yanagimoto, 1987; Yanagimoto, 1989).

Kuzumoto et al. (1990) simultaneously extruded two solutions containing the same polymer, but with different solvents and with the presence of additives to increase the permeability of the resulting membranes. The preparation of dual-layer hollow layer fibers, using two solutions with different polymers and extruded simultaneously through a triple extruder, was performed years later in patents developed by Ekiner et al. (1992) and Kusuki et al. (1992). In these works, a microporous inner layer and an anisotropic outer layer were obtained. An extremely thin dense skin in its superficial regions and porous intermediate layers were obtained. These fibers were used in gas separation tests.

The preparation of several other double layer hollow fibers with good performance for gas separation, consisting of different polymeric systems, were also presented in the literature (Suzuki et al., 1998; Kools, 1998; Sakashita et al., 1998; Pereira, 1999; Yang et al., 2001; Gomes, 2002; Jiang et al., 2004; DF Li et al., 2004; Y. Li et al., 2004). Suzuki et al. (1998), for example, prepared membranes for CO₂ / N₂ separation composed of a thin dense poly (imide) skin containing poly (ethylene oxide) and a porous layer based on another modified poly (imide). These fibers showed a permeability to CO₂ of 69.0 GPU with a selectivity of 33.0 in tests carried out at a temperature of 50.0 °C and one month after the fabrication of the membranes. However, the authors did not provide details about the design of the extruder used, nor information about the conditions of synthesis investigated and morphological structures obtained.

Most of the works in simultaneous processing of two polymer solutions, the phenomena and mechanisms responsible for the adhesion of the different obtained layers are not discussed in detail. The polymer concentration and the nature of the materials used in both layers (polymer, solvent, non-solvent and / or additives) can be highlighted as some determining factors for the accession. The use of solvent or solvent / non-solvent mixture in the two solutions may also be important, since the precipitation rates of both layers are changed. Adhesion is likely to be disadvantaged if precipitation of the skin and support layers are very different. It should be noted that the formation of delaminated layers can considerably affect the mechanical resistance of dual-layer membranes in high pressure permeation tests.

According to Pereira (1999), mass transfer and precipitation rate in the region close to the interface of the two solutions processed simultaneously can promote

the separation or interpenetration of the layers formed by the two solutions. It has been suggested that adhesion occurs between the layers when the region close to the interface remains stable for a enough to interpenetrate the solutions.

In another work, Li et al. (2002) identified that the concentration of the polymeric solution as well as the composition of the internal liquid, play an important role in obtaining dual-layer membranes free of delamination. Fluorinated poly (imide) and poly (sulfone ether) were the polymers used in the outer and inner layers, respectively.

Among the variables investigated by Duarte (2003), the use of both the same solvent in the preparation of the two solutions and an external coagulation bath, allowed a greater interpenetration between the layers of hollow fibers formed from solutions containing poly (urethane) and poly (sulfone). The use of a volatile solvent in the outer layer, different from that used in the internal solution, also allowed to obtain flat membranes and hollow fibers with complete adhesion between the resulting layers.

Jiang et al. (2004), studying the synthesis of hollow fibers composed of double layer based poly (imide) [matrimid, CIBA GEIGY] for external skin and poly (sulfone ether) as internal support, verified that the increase in the temperature of the extruder during spinning process improves the interpenetration between the two solutions, depending on the decreased viscosities and increased transfer rates between same. According to the authors, the flow rates of the two polymeric solutions they also significantly affect the adhesion between the resulting layers. They concluded that low flows from the external solution can cause defects in the

layers formed, while high flow rates of this solution can result in skin very thick and free of defects.

Some additional selected works are reported in Table 2.1., showing relevant results for the aim of the present research.

Table 2.1. Selected reported works and results on dual-layer membrane preparation

Author	Dense layer	Porous layer	Tested species	Results (compared to dense membrane)
Pereira <i>et al.</i> (2003)	Polyetherimide and polyethersulfone	Polyethersulfone	N/A	Non-homogeneous structure with some delamination between the layers
Carvalho, Roberto (2005)	Cellulose acetate	Polietherimide	NaCl solution (NF and RO)	Increased hidraulic permeability
Hashemifard <i>et al.</i> (2011)	Polyetherimide	Polysulfone	O ₂ , and N ₂	Permeability values were lower and selectivity remained the same
Braga Junior, Walter (2011)	Polyurethane	Polyethersulfone	Hexane, CO ₂ , and N ₂	Decrease in CO₂/N₂ selectivity with similar CO ₂ permeability values
Amaral, Rafael (2014)	Polyurethane	Polyethersulfone	CO ₂ , and N ₂	Decrease in CO₂/N₂ selectivity due to the presense of defects in the membrane

According to the reported results, although successfully dual-layer membranes were obtained, most of them showed a lower performance in terms of selectivity and/or permeability when compared to dense membranes. Therefore, there is a challenge in terms of achieving both homogeneous structure and good transport properties. Polyurethane in the dense layer and polyethersulfone in the support

layer appear to be a good combination for gas permeation with dual-layer membranes.

2.8. Mixed Matrix Membranes

Mixed Matrix Membranes (MMMs) are membranes constituted by two phases: a bulk phase (polymer matrix) and a dispersed phase (inorganic filler). These membranes can have higher permeability and selectivity because of the intrinsic transport properties of the inorganic filler (Chung et al., 2007).

Matavos-Aramyan *et al.* (2020) prepared nanocomposite membranes using polyurethane and polyesterurethane as polymers and silica as filler. They tested filler contents of 5, 10 and 15 wt%. It was found that for a Silica content of 15 wt%, CO₂ permeability decreased from 80 to 65 Barrer as a result of the reduction of diffusion passages through the polymer matrix. On the other hand, CO₂/N₂ selectivity increased from 30 to 38 due to the dissolving mechanism in the membrane, this being dominant in the presence of the silica nanoparticles and, as a result, enhancing CO₂ transport.

Weigelt *et al.* (2018) prepared mixed matrix membranes by combining the polymer Matrimid® 5218 and activated carbon (AC). They achieved AC contents up to 50 vol % in polymer matrix. They observed an increase of CO₂ permeability from 12.3 to 66 barrer for an AC volume fraction of 0.5 at 1000 mbar and 30 °C. Moreover, CO₂/CH₄ and O₂/N₂ selectivities showed a decrease from 36.8 to 29.7 and from 8.11 to 6.19, respectively.

Selected additional reports on the preparation of mixed matrix membranes are showed in Table 2.2.

Table 2.2. Selected reported works and results on mixed matrix membrane preparation.

Author	Polymer	Filler	Gases	Results
Weigelt et al. (2018)	Matrimid 5218	Activated carbon	H ₂ , He, CO ₂ , CH ₄ , O ₂ and N ₂	Permeability of all gases increased with CA content. Selectivity remained also constant
Cong et al. (2007)	poly(2,6-diphenyl-1,4-phenylene oxide)	Carbon nanotube	CO ₂ and N ₂	Enhanced CO₂ permeability with similar CO ₂ /N ₂ selectivity
Anson et al. (2004)	Acrylonitrile-butadiene-styrene	Activated carbon	CO ₂ and CH ₄ ,	Increase in CO₂ permeability and CO ₂ /CH ₄ selectivity
Wang et al. (2020)	Pebax	Silica (Functionalized)	CO ₂ and N ₂	Increased CO₂ permeability and CO₂/N₂ selectivity
Sunderhus, Aliny (2019)	Polyurethane	Silica (Functionalized)	CO ₂ , CH ₄ , O ₂ and N ₂	Both CO ₂ /CH ₄ and CO ₂ /N ₂ selectivities increased with similar permeability values
Matavos-Aramyan et al. (2020)	Polyurethane and polystyrene	Silica	CO ₂ O ₂ and N ₂	Permeability for all gases decreases and CO ₂ /N ₂ and O ₂ /N ₂ selectivity increased
Fioravante, Carolina (2016)	Polyurethane	Ag nanoparticles	Propylene, propane	Increased permeability for both species and reduction in the selectivity values.
Molki et al. (2019)	Polyurethane	Nickel Oxide	CO ₂ , CH ₄ , O ₂ and N ₂	CO ₂ /N ₂ selectivity increased and CO ₂ permeability remained almost constant

As it can be seen, in all of these works, the addition of silica or activated carbon into the polymer matrix resulted in the enhancement of CO₂ permeability and selectivities. Also, polyurethane appears to be a good material to incorporate nanoparticles due to its structure with both rigid and flexible chains.

2.9. State of the art and this research proposal

Based on the fundamentals and on recent articles described in previous sections, this Thesis will investigate further dual-layer membrane preparation by the co-casting technique. Polyurethane is used for the dense layer because of its performance on CO₂ removal; and polyethersulfone for the porous layer due to its mechanical properties. Although there are several previous articles reporting the use of this technique, there is still some difficulty in obtaining good adhesion and homogeneity in the layers. Because of this, it is important to study some of the variables in this technique and their effect on the membrane structure. This work aims to evaluate some of those variables in order to prepare dual-layer membranes with improved adhesion and homogeneity. Also, the membranes are tested in a gas permeation process to evaluate the effect of pressure and temperature on their performance in CO₂ capture from flue gas.

Moreover, the literature shows the importance of enhancing the performance of the membranes in terms of permeability and selectivity. The use of nanoparticles into the polymer matrix has become a common alternative in order to get higher permeability and selectivity in the membranes. However, most of those works are focused on dense membranes or porous membranes (only one layer). This Thesis proposes the addition of two different nanoparticles (activated carbon and silica) into the dual-layer membranes aiming to improve their performance in CO₂ capture from flue gas. The effect of the kind of nanoparticle and the content in the polymer matrix will be evaluated.

.

3. Polyurethane/Polyethersulfone dual-layer anisotropic membranes for CO₂ removal from flue gas

First published In J Appl Pol Sci, 20 January 2021 <https://doi.org/10.1002/app.50476>

ABSTRACT

Removing CO₂ from flue gas streams has been a permanent challenge regarding environmental issues. Membrane technology is a solution for this problem but more efficient membranes are required. The fabrication of dual-layer polyurethane / polyethersulfone membrane by the co-casting technique is undertaken and the effects of previous evaporation time and coagulation water bath temperature on membrane morphology are explored. Uniform layers with excellent adhesion are obtained. The effect of feed pressure and temperature on membrane permeability and selectivity for CO₂, N₂ and O₂ are studied. Increasing the pressure from 1 - 8 bar results in a reduction of CO₂ permeability and CO₂/N₂ ideal selectivity from 19.6 to 13.0 Barrer, and from 66 to 60, respectively. Temperature in the range of 25 - 45 °C enhances CO₂ permeability from 19.6 to 28.9 Barrer, although CO₂/N₂ selectivity decreases from 66 to 43, yet showing good potential for applications.

INTRODUCTION

Dual-layer polymeric membranes have been used for CO₂ removal from natural gas, H₂, and flue gas streams (Hwang et al., 2013, 2014a; Jin Yoo et al., 2018; Yoo et al., 2018). These membranes are formed by at least two layers: one selective layer for species separation and one support (non-selective) layer to achieve mechanical properties requirements. This membrane morphology allows the use of different material in each layer, making possible to combine both high permeability and selectivity, and at the same time to save materials used in the selective layer. There are several methods to prepare dual-layer membranes, among them, the co-casting of two solutions, which reduce the preparation time and allows the use of solvents that can dissolve both polymers used in the fabrication process (Hashemifard et al., 2011b; Karimi & Hassanajili, 2017b; X. M. Li et al., 2010b). However, the adhesion of layers of different materials plays an important role in dual-layer membrane preparation (X. M. Li et al., 2010a; Naderi et al., 2019; Ullah Khan et al., 2018b; Xia et al., 2018a). Several polymers have been used for CO₂ removal, especially those with high solubility of polar gases (Isfahani, Sadeghi, et al., 2016). Among rubbery polymers, polyurethane (PU) has showed high selectivity and versatility for CO₂ removal from flue gas (Choi et al., 2017; Isfahani, Ghalei, et al., 2016; Sadeghi et al., 2011; Ullah Khan et al., 2018b). For the non-porous layer, polyethersulfone (PES) is widely used because of its good mechanical properties and adhesion with several polymers used as materials for the selective layer (Fu et al., 2014; X. M. Li et al., 2010c; Lillepärq et al., 2019; Pereira et al., 2001).. Furthermore, polyvinylpyrrolidone has been frequently included into PES dope solutions to control the support layer

porosity and, in case of co-casting, to improve adhesion between both layers (Fu et al., 2014; X. M. Li et al., 2010c; Wu et al., 2018)

PU and PES may be dissolved in common solvents, which suggest that the co-casting method has good potential to prepare dual-layer membranes. Pereira et al.¹⁸ prepared dual-layer membranes using a solution of tetrahydrofuran (THF) and N-methyl-2-pyrrolidone (NMP) as solvent for the selective dope and NMP for the porous layer dope. PEI and PES were used for both the porous and selective layer. They investigated the exposure time (prior to immersion) of the casted solutions, including its effect on membrane morphology. However, the membranes did not show good adhesion and homogeneity. Mei-Li et al. (2016) studied delamination in polyetherimide/polysulfone dual-layer membranes by using NMP as solvent for both dope solutions to improve adhesion between the layers. They found that, to improve adhesion between the layers, both of them should shrink proportionally with closer percentage values upon coagulation.

Few reports are available on the co-casting process for dual-layer membrane preparation using a PU as selective layer. In this work, flat sheet dual-layer membranes were prepared by the co-casting method using PU/THF and PES/PVP/NMP as dope solutions for the selective and porous layer, respectively. To the best of our knowledge, this is the first work to obtain and evaluate homogeneous flat sheet PU dual-layer membranes by this method, aiming at CO₂ removal from flue gas.

EXPERIMENTAL

Materials

Tetrahydrofuran (THF) from Merck and polyurethane (PU) Ellastollan® from Basf were used for both the selective layer and dense membrane dope solutions. Polyethersulfone (PES) (ULTRASON E6020) and N-methyl-2-pyrrolidone (NMP) from Basf were used for the porous layer dope solution. Polyvinylpyrrolidone (PVP-K90) from Fluka was used as additive for the PES/NMP solution. Standard CO₂, N₂ and O₂ from Linde Gases Brasil were used with purity of 99.99%.

Membrane Preparation

For dense membranes 10 wt% of PU was dissolved in THF by stirring at 40 °C for 24h and then, cooled to 25 °C. The solution was poured on a Teflon petri dish and dried at 25 °C for 72h. The obtained membrane was taken to an oven at 60 °C for 12h to remove the residual solvent ¹⁴.

For the dual-layer membrane, two solution dopes were considered: the previously used PU/THF (10/90 wt%) and a PES/PVP/NMP (15/5/80 wt%) for the selective and support layer, respectively. A PES/NMP solution was first prepared and stirred at 50 °C for 24h. Then, PVP was added, stirring for additional 24h at the same temperature until total dissolution. The dual-layer membrane was prepared by the NIPS (non-solvent induced phase separation) method by using the co-casting process ⁸. The support layer solution was cast on a glass plate followed by the casting of the selective layer solution. The cast thickness for each solution was approximately 120 µm. Then, the cast dual-layer film was exposed to the environment at 25 °C to allow THF partial evaporation. The glass plate was then submerged for 30 min in distilled water to induce phase separation leading

to membrane formation. The membrane was kept in fresh water bath at room temperature for 48h to remove residual NMP, and finally dried at room temperature.

Scanning Electron Microscopy

Scanning Electron Microscopy (SEM) Vega (Tescan 3) was used to characterize the morphology and thickness of the dense and dual-layer membranes. Scanning Electron Microscopy integrated with Energy Dispersive X-Ray Spectroscopy (SEM/EDS) Vega (Tescan 3) was used to investigate the polymer distribution in both layers. The thicknesses of each layer were averages values of measures taken in ten different locations in the samples.

Gas permeation measurement

The permeance of pure gases (CO_2 , N_2 and O_2) for the dense and dual-layer membranes was evaluated using the permeation system described in Figure 3.1.

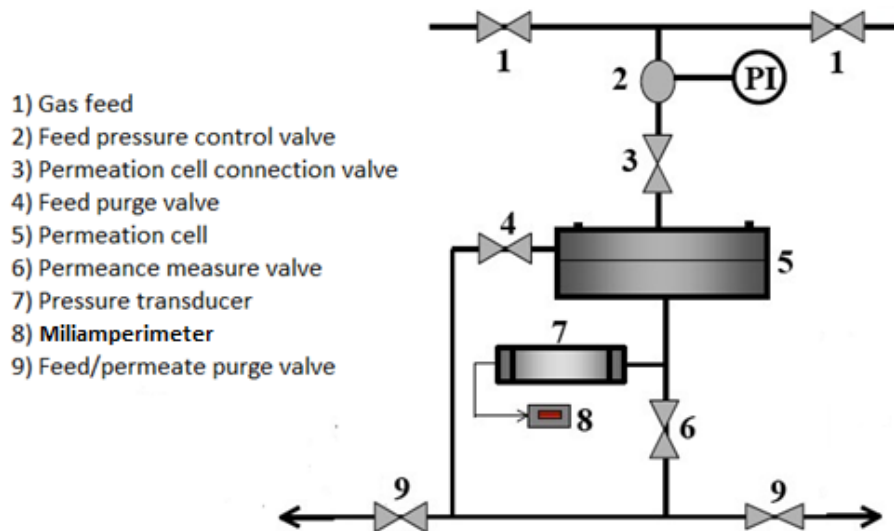


Figure 3.1. Diagram of the permeation system for pure gases

Each sample was sealed into a cylindrical cell with an effective membrane area of 8.5 cm². Before the test, the pressure was increased in the feed side in order to achieve a specific pressure difference through the membrane. During the test, the pressure variation data in the permeate side was recorded using the software LogChart II until reaching a permanent linear behavior. Gas permeance was calculated with equation (3.1).

$$L = \left(\frac{T_{STP}}{T P_{STP}} \right) \left(\frac{V_d}{A \Delta P} \right) \left(\frac{dP}{dt} \right)_{SS} \quad (3.1)$$

where L is the permeance in GPU (1 GPU = 1 x 10⁻⁶ cm³ (STP) / cm² s cmHg), T_{STP} and P_{STP} are the temperature and pressure at standard conditions, T is the permeation temperature (K), V_d is the downstream volume (cm³), A is the effective area of the membrane in the cell (cm²), ΔP is the pressure difference between the feed and permeate sides, $\left(\frac{dP}{dt} \right)_{SS}$ is the steady state pressure rate in the downstream chamber.

The ideal selectivity $\alpha_{A/B}$ was calculated with equation (2).

$$\alpha_{A/B} = \frac{P_A}{P_B} \quad (3.2)$$

P_A and P_B are the permeability (or permeance) values for the component A and B, respectively.

RESULTS AND DISCUSSION

Effect of the water bath temperature

Fig 3.2 shows photomicrographs of the cross-section of the dual-layer membranes obtained with different water bath temperatures without evaporation prior to immersion.

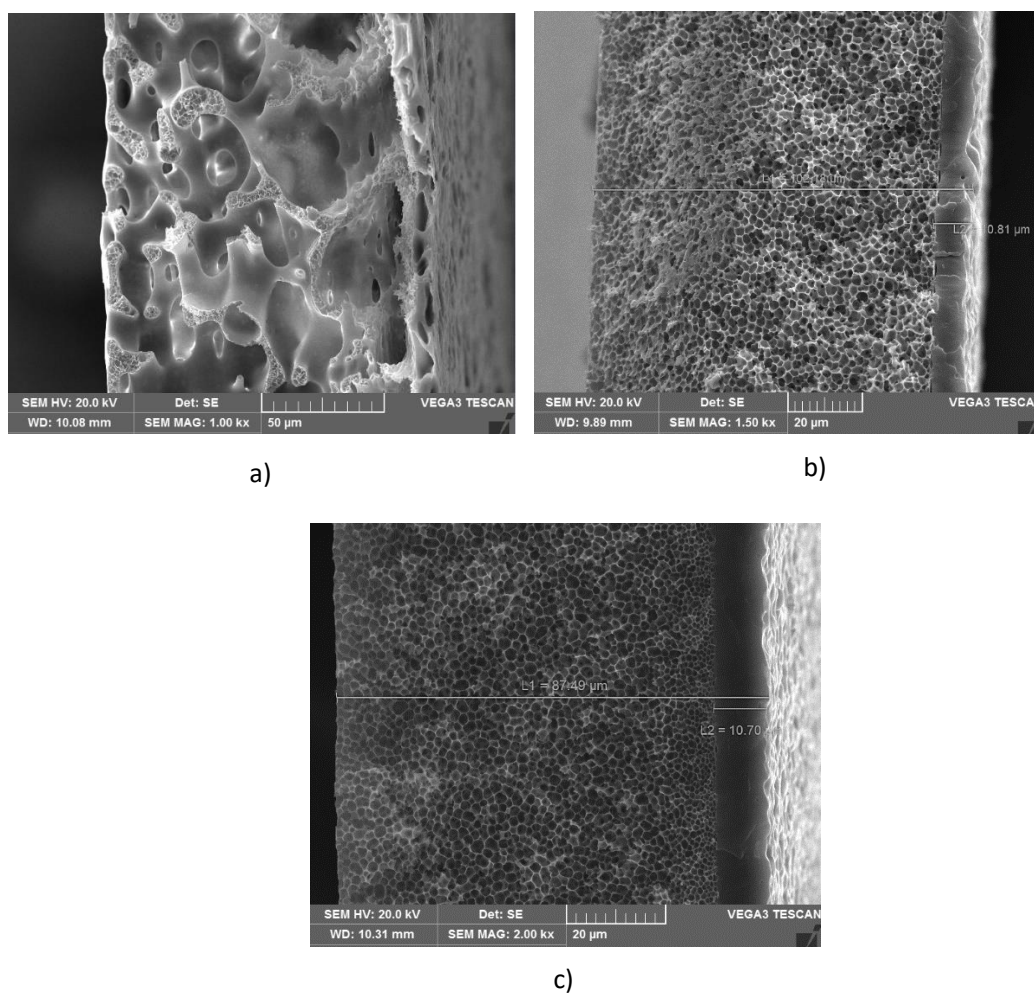


Fig 3.2. Cross-sectional images of the dual-layer membranes prepared using different water bath temperatures: a) 25 °C, b) 50 °C, c) 75 °C.

In order to better understand the effect of the water bath temperature and exposure time on membrane morphology and adhesion, Fig 3.3 shows the most expected and relevant fluxes through the interface during the exposure time and during the immersion into the water bath.

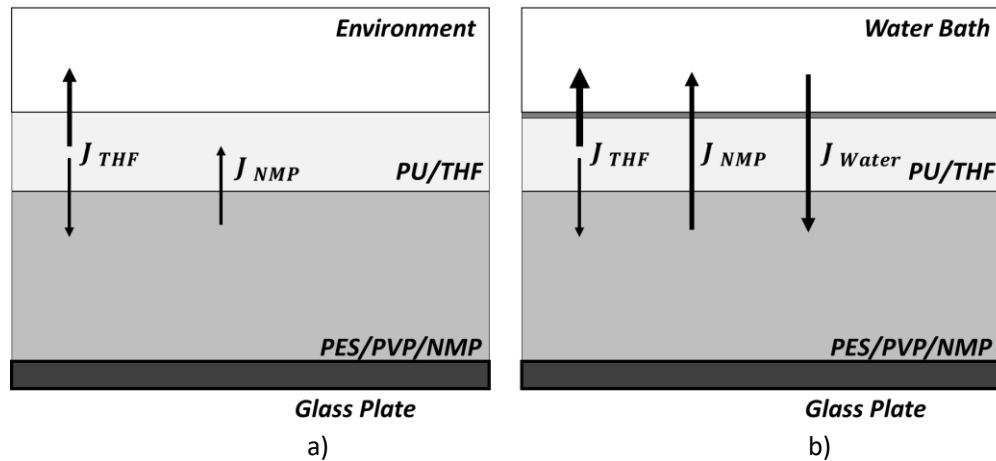


Fig 3.3. Membrane formation: expected fluxes in the co-casting process during a) exposure to environment, b) immersion in water bath.

As THF is volatile, a thin concentrated PU solution layer on the surface will be formed prior to the immersion into the water bath. In addition, a flux of NMP will be established from the PES dope towards the upper PU dope, maintaining homogeneity of this layer. However, this flux is probably negligible compared to evaporating THF flux. As exposure proceeds, a thin denser PU layer is formed on the surface (Fig 3.3b). Upon immersion in the water bath, the remaining THF in the PU dope is extracted and the selective layer solidifies. On the other hand, the hydrophilic NMP migrates outwards through the PU layer, while a water flux increase in the opposite direction, towards the PES dope. There, in this sublayer, phase separation occurs and the PES porous structure is generated.

The photomicrograph of Figure 3.2a shows that a coagulation bath at 25 °C resulted into a one-phase porous membrane. Since there is an affinity between polymers and solvents used in both solutions, the slower mass transfer during precipitation allowed the mixing of both cast solutions during the membrane formation process. There is enough time to reach homogeneity before polymer precipitation. However, when the water bath temperature was increased, one can expect higher mass transfer rates, hence conditions for polymer precipitation, leading then to the two distinct layers. In Fig. 3.2b, it is possible to observe a very well-defined interface between both layers. Furthermore, there is an effect on the shrinkage percentage of each layer, calculated as a ratio between the thickness before and after membrane precipitation for each layer. A higher flux of NMP reduces the shrinkage difference between both layers during the membrane formation, which allows better adhesion. However, for a coagulating bath at 75 °C, the depleted THF mass transfer is so fast that it cannot avoid some phase separation, resulting in a rough non-homogeneous surface top layer, as it can be seen in the Fig 2 (c). In order to get a more uniform surface, it is necessary to reduce the THF mass transfer rate outwards the water bath. This can be achieved by previously allowing a THF partial evaporation, which favors a more concentrated PU layer at the surface before immersion.

Effect of evaporation time

The effect of evaporation time on membrane structure can be seen in Fig 3.4 where cross sections of dual-layer membranes prepared by immersion in a water bath at 75 °C are shown.

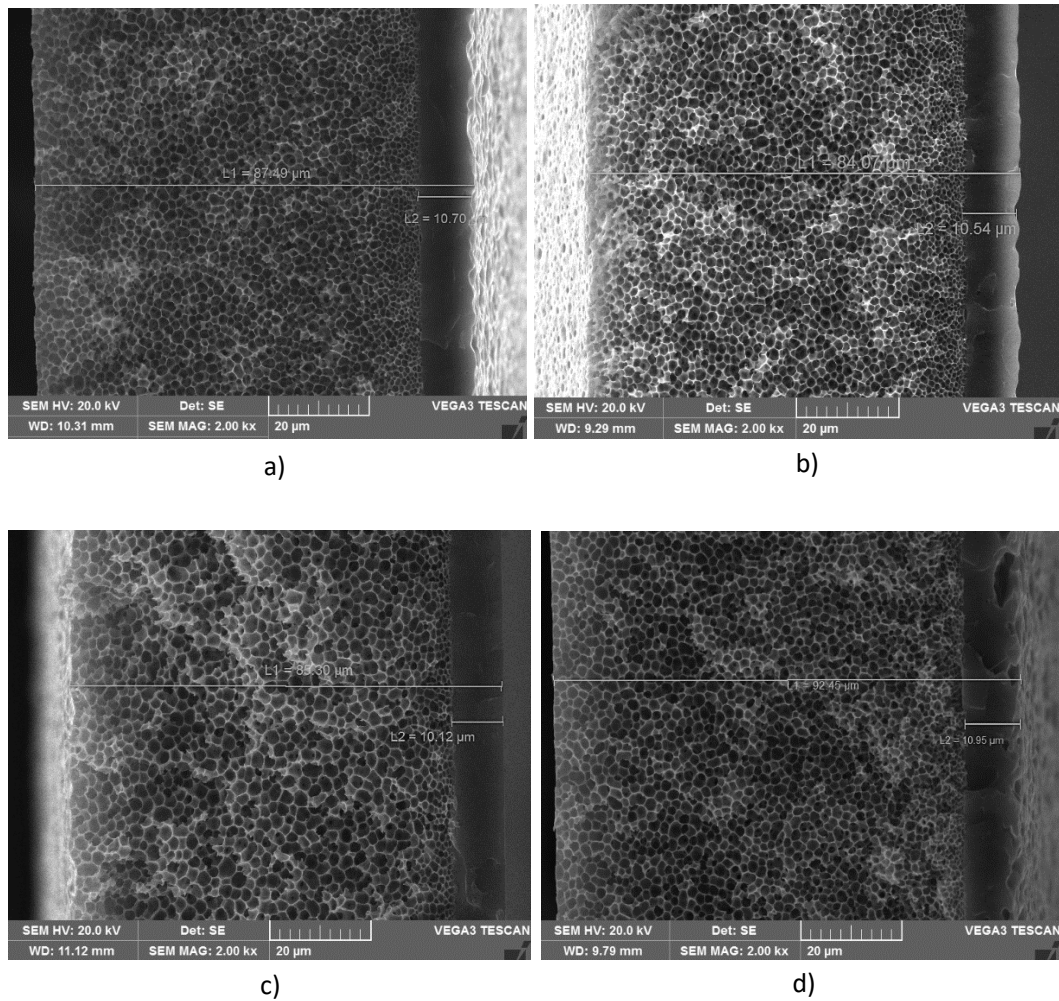


Fig 3.4. Cross-sectional images of the dual-layer membranes prepared using different exposure times: a) No evaporation b) 5 s c) 15 s d) 30 s.

As it is shown in the Fig 3.4, increasing the evaporation time allowed to get a more uniform surface. Since the dense layer formed as result of the THF evaporation creates an additional barrier between the water and the cast solutions, the THF mass transfer rate towards the coagulation bath is lower, resulting in a more uniform surface. Also, for an evaporation time of 15 s, the shrinkage difference between the porous and dense layer was reduced (from 27 - 91% to 29 - 91% for evaporation times of 0 and 15 s, respectively), which enhances adhesion between the layers as it was seen in the previous section.

However, for higher evaporation times (30 s), some defects are created in the dense layer. This time was probably enough to allow the entrance of NMP from the porous solution into the dense solution. Thus, when submerged into the coagulation bath, the presence of NMP in the dense layer led to a phase separation process, creating some pores across that layer.

Fig 3.5 shows the cross-sectional images using Energy Dispersive X-Ray Spectroscopy (EDS). Sulfur is the reference element because it is the one that should exist only in the porous layer (PES).

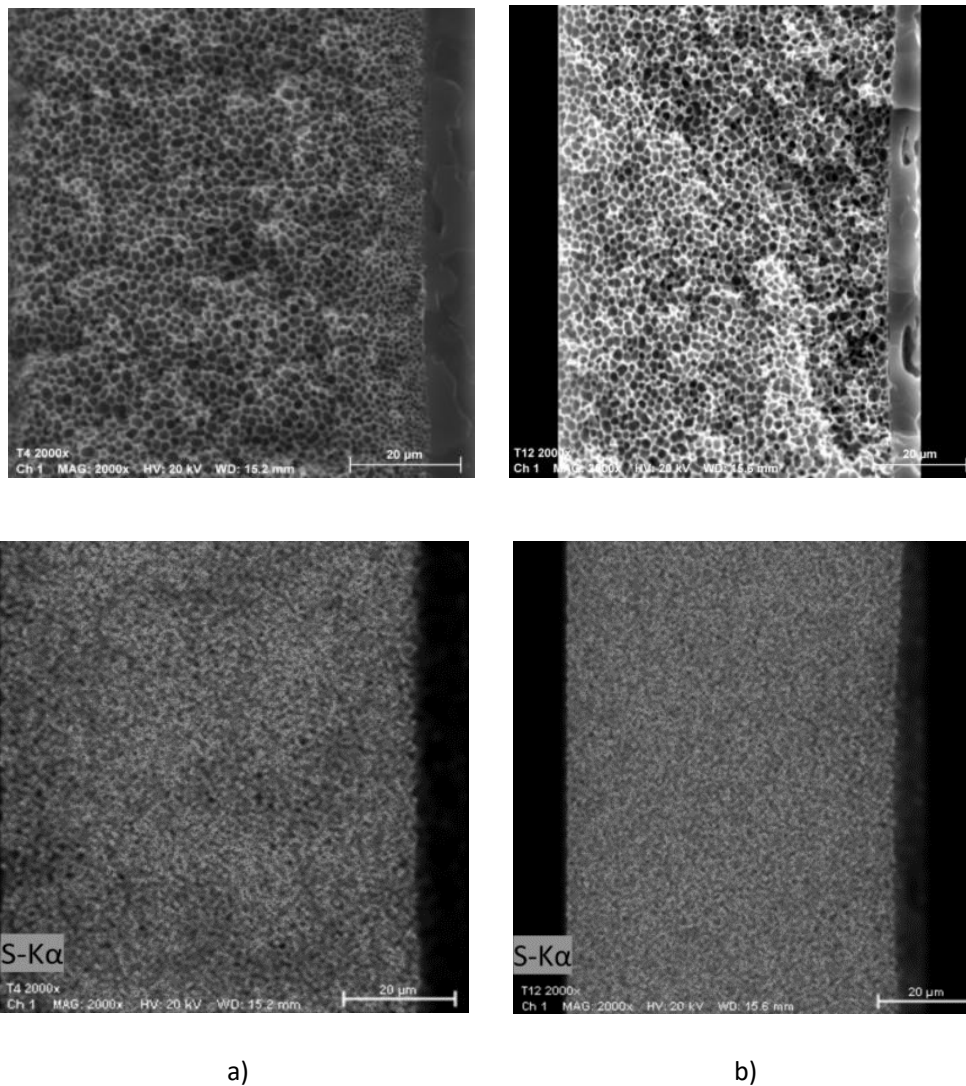


Fig 3.5. Cross-sectional images (Energy Dispersive X-Ray Spectroscopy – EDS) of the dual-layer membranes prepared with different exposure time: a) 15 s, b) 30 s.

It can be seen that for 15 s of exposure, there was no sulfur in the dense layer, so no mixing of the dopes happened before membrane formation and both layers were completely well-defined and uniform. However, for an exposure time of 30 s, sulfur was detected in the dense layer, which is a strong indication that, during the evaporation, there is a diffusion outwards of the lower solution, mixing with the PU more concentrated solution. Exploring other fabrication factors such as temperature of the solutions and partial pressures of solvents in the environmental air should provide means to reduce transfers rate between the solutions even at higher evaporation times.

Gas permeation results

Permeation of pure CO₂, N₂ and O₂ for dense and dual-layer membranes were performed. The selected dual-layer membranes were prepared with an evaporation time and coagulation bath temperature of 15 s and 75 °C, respectively. Both dense and dual-layer membrane had a total thickness of 85 μm (±1 μm), with a dense layer thickness of 10 μm (±0.2 μm) in the dual-layer membrane. All tests were performed in triplicate and the results are shown in Table 3.1.

The permeability values showed in Table 1 were considering the thickness of the dense layer, taken from the SEM images (85 μm and 10 μm for the dense and dual-layer membranes, respectively).

Table 3.1. CO₂ permeability and ideal selectivity for PU dense and PU/PES dual-layer membranes. Feed pressure = 1 bar, Temperature = 25 °C.

Membrane	P _{CO₂} (Barrer)	P _{N₂} (Barrer)	P _{O₂} (Barrer)	α _{CO₂/N₂}	α _{O₂/N₂}
Dense	41	0.60	1.03	68.20	1.71
Dual-layer	19.62	0.30	0.51	66.06	1.71

One can observe that CO₂ permeability was about twice higher in the dense membrane when compared to the dual-layer. This can be attributed to the additional resistance given by the porous layer in the dual-layer membrane, as it can be estimated by the conventional resistance model of Equation (3).

$$R_T = R_{DL} + R_{PP} + R_{PL} \quad (3)$$

Where R_T is the total resistance, R_{DL} is the dense layer resistance, R_{SL} is the resistance given by the fraction of the dense layer that penetrated the pores and R_{PL} is the porous layer resistance. According to the SEM images, R_{PL} can be assumed negligible, resulting into:

$$\left(\frac{P}{l}\right)_T = \left(\frac{l_{DL}}{P_{DL}} + \frac{l_{PL}}{\varepsilon P_{PL}}\right)^{-1} \quad (4)$$

where $\left(\frac{P}{l}\right)_T$ is the permeability in the dual layer membrane at temperature T and ε is the porosity of the porous layer. By solving this equation for any of the gases, it is possible to estimate the porosity to know the additional resistance given by the porous support. For CO₂, with an intrinsic permeance of 12 GPU for the PES, the estimated porosity is 0.12. Since the support porosity is low, there is a high mass resistance in the support layer resulting in lower permeability in the dual-layer membrane, as it can be seen in Table 3.1. The small difference in the CO₂/N₂ selectivity between dense and dual-layer membranes can be explained by the combination of two effects. First, CO₂ permeance in PES is higher than in PU so mass transport rate of this gas through the polymer matrix in the porous support is higher. Also, the kinetic diameter of CO₂ is smaller when compared to N₂ (3.30 and 3.64, respectively), therefore CO₂ mass transport rate through the porous structure is enhanced.

Moreover, Figure 3.6 shows the 2008 Robeson diagram for membranes in CO₂/N₂ separation and the location of the dual-layer membranes of this work into the diagram.

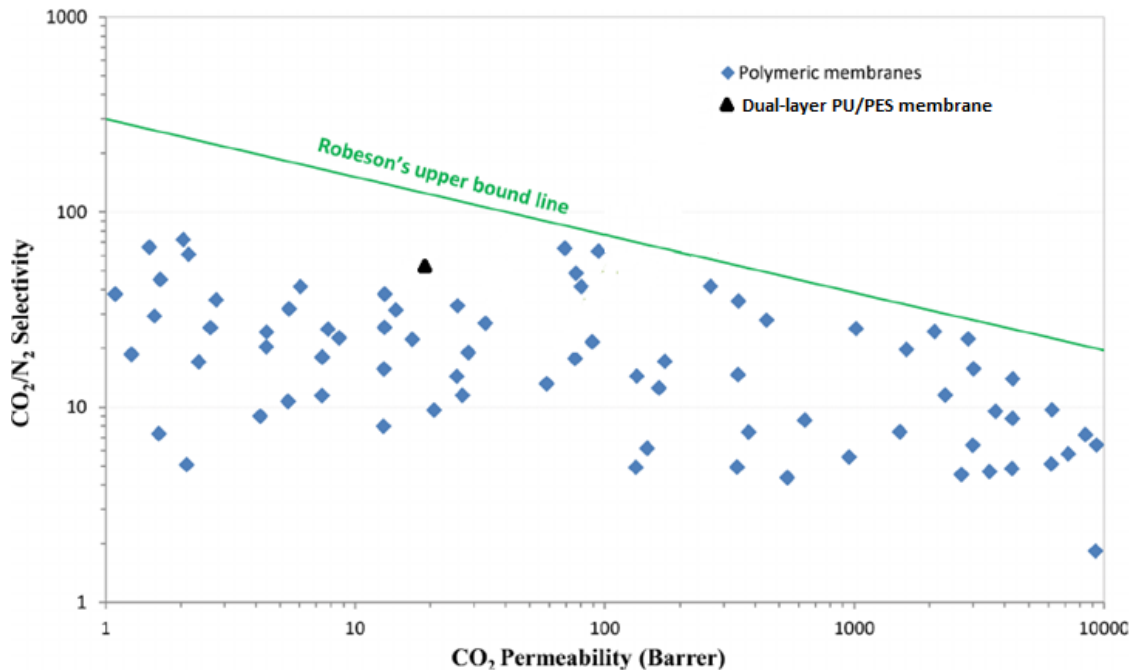


Fig 3.6. PU/PES dual-layer membranes in the 2008 Robeson diagram.

As it can be seen, the PU/PES dual-layer membranes showed a high permeability when compared with most of the polymeric membranes in the diagram. However, their performance in terms of CO₂ permeability is still low so it is necessary to enhance CO₂ transport through the membrane. This could be achieved by the addition of an inorganic filler into the polymer matrix in order to favor CO₂ sorption and/or diffusion in the membrane (Matavos-Aramyan et al., 2020; Weigelt et al., 2018).

Effect of pressure difference on permeance

Permeation tests were performed for membrane pressure differences of 1, 2, 4 and 8 bar at 25 °C and an estimated porosity value was calculated for each condition.

Table 3.2. Effect of pressure difference on gas permeation for the dual-layer membranes. Temperature = 25 °C.

Pressure (bar)	P_{CO₂} (Barrer)	P_{N₂} (Barrer)	P_{O₂} (Barrer)	α_{CO₂/N₂}	α_{O₂/N₂}	Porosity (ε)
1	19.62	0.30	0.51	66.06	1.71	0.12
2	17.42	0.28	0.48	62.89	1.74	0.12
4	14.77	0.25	0.46	60.29	1.88	0.12
8	13.01	0.22	0.42	59.95	1.95	0.11

As it is shown in Table 3.2, the permeability of all gases decreased with pressure. To explain this behavior, it is important to take into account that, for both dense and dual-layer membranes, the permeability for each depends mainly on the solubility and diffusion of each component through the selective layer (PU in this case). However, the pressure has two opposite effects on diffusion. First, due to the higher gas concentration in the polymer matrix, the free volume in the membrane increases; on the other hand, as pressure over the membrane increases, compression of the polymer chains and reduction of the free volume may occur. In rubbery polymers, the second effect is often more relevant due to the more flexible chains, therefore diffusion tends to decrease with feed pressure. So, for higher pressures, gases with higher kinetic diameter will be more restricted to pass through the membrane²⁰. Thus, the expected effect of pressure on permeability should be in the order CO₂ < O₂ < N₂, however the results showed another pattern, namely O₂ < N₂ < CO₂. In rubbery polymers, CO₂ permeability is highly dependent on its solubility into the polymer matrix²¹. CO₂ interaction with

PU is favored because of its polarity and interaction with PU groups. Hence, its solubility is more affected by pressure difference, resulting in lower permeability values.

Effect of temperature on permeance

Permeation tests were performed for temperatures of 25, 35 and 45 °C at 1 bar and the results are showed in Table 3.3.

Table 3.3. Effect of water temperature on gas permeation for the dual-layer membranes. Pressure = 1 bar.

Temperature (°C)	P_{CO₂} (Barrer)	P_{N₂} (Barrer)	P_{O₂} (Barrer)	α_{CO₂/N₂}	α_{O₂/N₂}
25	19.60	0.30	0.51	66.06	1.71
35	23.10	0.43	0.69	53.69	1.61
45	28.90	0.67	0.96	43.34	1.45

Increasing temperature resulted in higher permeance values for all the gases in both dense and dual-layer membranes. This happened due to the increasing of the free volume with temperature, which facilitated the transport of the gases through the membrane. Moreover, since N₂ has a higher molecular size, the increasing in its permeability is more enhanced, resulting in a reduction of CO₂/N₂ and O₂/N₂ selectivity.

CONCLUSIONS

Dual-layer PU/PES membranes aiming at CO₂ removal from flue gas were successfully prepared by the co-casting method. It was possible to prepare dual-layer membranes using two different materials with similar solvent affinity. The effects of the coagulating bath temperature and solvent evaporation time were established and showed that a good layers adhesion and an homogenous support structure were obtained for a 15 s evaporation time and a water coagulating bath at 75 °C as observed by SEM.

The normalized effective permeability (permeance/thickness of dense layer) of single components CO₂, N₂ and O₂ was calculated for both dense PU and dual-layer PU/PES membranes. Permeance values were higher for the dual-layer membranes but, since the porous support provides an additional mass resistance to the membrane, the permeability values for the dual-layer were lower. Permeation tests in the ranges of 1-8 bar for feed pressures showed a decrease of permeability for all gases. CO₂/N₂ ideal selectivity decreased from 66 to 60 in that pressure range since CO₂ solubility into PU was more affected. On the other hand, tests performed in the range of 25-45 °C showed an enhancement of gas permeability with temperature due to a higher free-volume available in the dense layer. However, since the effect is more important for gases with higher kinetic diameter (N₂), the CO₂/N₂ selectivity decreased from 66 to 43 in that temperature range. The optimization of the co-casting method should prove useful for the fabrication of selective dual-layer membranes aimed at gas separation, allowing the use of versatile pairs of materials for the layers.

4. Polyurethane/Polyethersulfone mixed matrix dual-layer membranes containing inorganic particles for CO₂ removal from flue gas

Submitted 09 February 2021 to Journal of Applied Polymer Science (Under revision)

ABSTRACT

CO₂ removal from flue gas has become an important challenge in order to reduce global warming. Gas permeation with dual-layer membranes is a solution for this problem but membranes with better performance are necessary. The fabrication of mixed matrix dual-layer membranes is undertaken with two different fillers: activated carbon and silica. The effects of the filler content on membrane morphology are explored. The adhesion and homogeneous structure of the layers are maintained for lower filler content. The effect of feed pressure (1 – 8 bar) on membrane permeability and selectivity for CO₂, N₂ and O₂ is studied. At 1 bar, the presence of activated carbon and silica enhances CO₂ permeability from 19.6 to 22.6 and 23.1 Barrer, respectively. Moreover, higher feed pressure values lead to an increase of more than 40% in CO₂ permeability for the membranes with activated carbon, showing good potential for flue gas treatment.

INTRODUCTION

Atmospheric CO₂ level is one of the most important causes of climate change. In order to reduce emissions, CO₂ capture has become a necessary intervention (Meihong Wang et al., 2015; Zhang et al., 2013; Zhao et al., 2016). Recently, membrane processes have been widely used for this application with the use of thin film composite membranes for CO₂ removal from natural gas, H₂, and flue gas (Hwang et al., 2013, 2014b; Jin Yoo et al., 2018; Yoo et al., 2018). These membranes are formed by at least two layers: one selective layer for species separation and one support (non-selective) layer to ensure the mechanical properties requirements. This membrane morphology allows the use of different material in each layer, allowing a combination of both high permeability and selectivity (Hashemifard et al., 2011b; Ullah Khan et al., 2018a; Xia et al., 2018a). Moreover, it is possible to incorporate inorganic nanoparticles into the selective layer to increase its performance. These membranes are called mixed matrix membranes (MMMs) and combine the advantages and versatility of the polymeric membranes with the separation properties of the inorganic materials (Afarani et al., 2018; Brunetti et al., 2017; Molki et al., 2018; Sabetghadam et al., 2019; Ming Wang et al., 2017). The inorganic fillers can be solid (impermeable) or porous (permeable). Activated carbon is a versatile porous filler used for CO₂ capture because of its high surface area and pore size distribution. On the other side, the use of silica as a solid filler has resulted into an enhancement of membrane permeability in CO₂ capture processes (Vinoba et al., 2017). An alternative procedure to prepare a thin film composite membrane is co-casting of two different polymer solutions, to obtain the so-called dual layer membranes⁸⁻¹⁰. This technique allow the use of polymers that are miscible in a

same solvent, increasing the alternatives of polymer choice and reducing the number of preparation steps. However, adhesion between polymer layers is the main issue to be controlled during membrane preparation. In a previous study, polyurethane/polyethersulfone (PU/PES) dual-layer membranes were successfully prepared by the co-casting process (Garcia Jiménez et al., 2021). It was possible to obtain membranes with uniform morphology and good adhesion between the layers.

Aiming to improve PU/PES dual layer membranes performance (permeability and selectivity), this work explores the preparation of novel dual-layer MMMs. Activated carbon and silica were chosen as porous and solid fillers, respectively. The effect of filler content on membrane morphology and performance was evaluated at different feed pressures.

EXPERIMENTAL

Materials

Tetrahydrofuran (THF) from Merck and polyurethane (PU) Ellastollan® from Basf were used for both the selective layer and dense membrane dope solutions. Polyethersulfone (PES) (ULTRASON E6020) and N-methyl-2-pyrrolidone (NMP) from Basf were used for the porous layer dope solution. Polyvinylpyrrolidone (PVP-K90) from Fluka was used as additive for the PES/NMP solution. CO₂, N₂ and O₂ from Linde Gases Brasil were used with purity of 99.99%. Activated carbon (Conocco Phillips) and Silica (Aerosil 200, Degussa-Hüls) were used as inorganic particles with an average size of 300 nm and 12 nm, respectively.

Membrane Preparation

Two solution dopes were considered: the previously used PU/THF (10/90 wt%) and a PES/PVP/NMP (15/5/80 wt%) for the selective and support layer, respectively (Garcia Jiménez et al., 2021). In the case of MMMs, to avoid agglomeration, the filler was first dispersed into THF and ultra-sonicated at 60 Hz for 30 min. Then, it was mixed with the PU-THF solution (already dissolved) and stirred for 1 h to make a homogeneous solution.

The dual-layer membrane was prepared by the NIPS (non-solvent induced phase separation) method by using the co-casting process⁸. The support layer solution was cast on a glass plate simultaneously with the casting of the selective layer solution. The cast thickness for each solution was approximately 120 μm and the dual-layer film was exposed to the environment (relative humidity 60%, 25°C) during 15 s to allow THF partial evaporation. The glass plate was then submerged for 30 min in distilled water at 75 °C to induce phase separation

leading to membrane formation. The membrane was kept in fresh water bath at room temperature for 48h to remove residual NMP, and finally dried at room temperature. Table 4.1 shows the membranes prepared in this study and the expected particle content in the dense layer for each one. This value was calculated assuming that there was no loss of particle or polymer into the water bath during membrane precipitation.

Table 4.1. Dense layer particle content in the PU/THF (10/90 wt%) dope formulation in the preparation of composite membranes. AC – Activated carbon; SI – Silica

Membrane	Particle	Content (%wt)*
M-0	none	0
M-AC1	Activated Carbon	1
M-AC2	Activated Carbon	2
M-AC5	Activated Carbon	5
M-SI1	Silica	1
M-SI2	Silica	2
M-SI5	Silica	5

*Particle content based on polymer mass

Scanning Electron Microscopy

Scanning Electron Microscopy (SEM) Vega (Tescan 3) was used to characterize the morphology and thickness of the dense and composite membranes. Scanning Electron Microscopy integrated with Energy Dispersive X-Ray Spectroscopy (SEM/EDS) Vega (Tescan 3) was used to investigate the silica distribution through the membrane and to estimate its composition in the dense layer. The thickness of each layer in the composite membrane was an average value taken from ten different locations in the samples.

Gas permeation measurement

The permeance of pure gases (CO₂, N₂ and O₂) in the dense and composite membranes was evaluated using the permeation system described in Figure 4.1 operated in transient mode, following the permeate build up pressure.

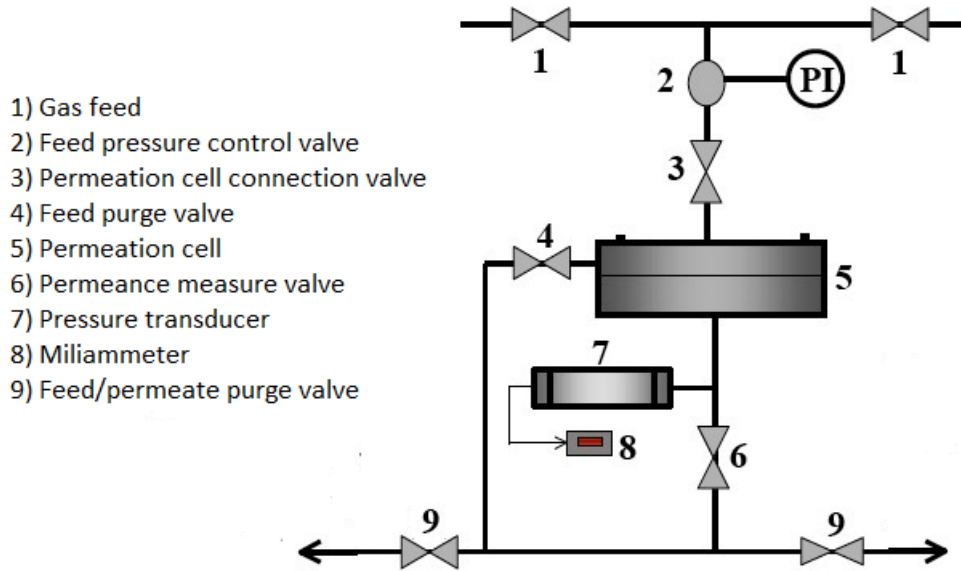


Figure 4.1. Diagram of the permeation system for pure gases

Each sample was sealed into a circular cell with an effective area of 8.5 cm². Pressure was initially increased in the feed side in order to reach a specific pressure difference through the membrane. During the measurement test, the pressure variation data in the permeate side was collected by using the software LogChart II. Gas permeance was calculated with equation (4.1).

$$L = \left(\frac{T_{STP}}{T P_{STP}} \right) \left(\frac{V_d}{A \Delta P} \right) \left(\frac{dP}{dt} \right)_{SS} \quad (4.1)$$

L is the permeance in GPU (1 GPU = 1 x 10⁻⁶ cm³ (STP) / cm² s cmHg), T_{STP} and P_{STP} are the temperature and pressure at standard conditions, T is the permeation temperature (K), V_d is the downstream volume (cm³), A is the

effective area of the membrane in the cell (cm^2), ΔP is the pressure difference between the feed and permeate sides, $\left(\frac{dP}{dt}\right)_{SS}$ is the steady state pressure increase rate in the downstream chamber.

Ideal selectivity $\alpha_{A/B}$ was calculated with equation (4.2).

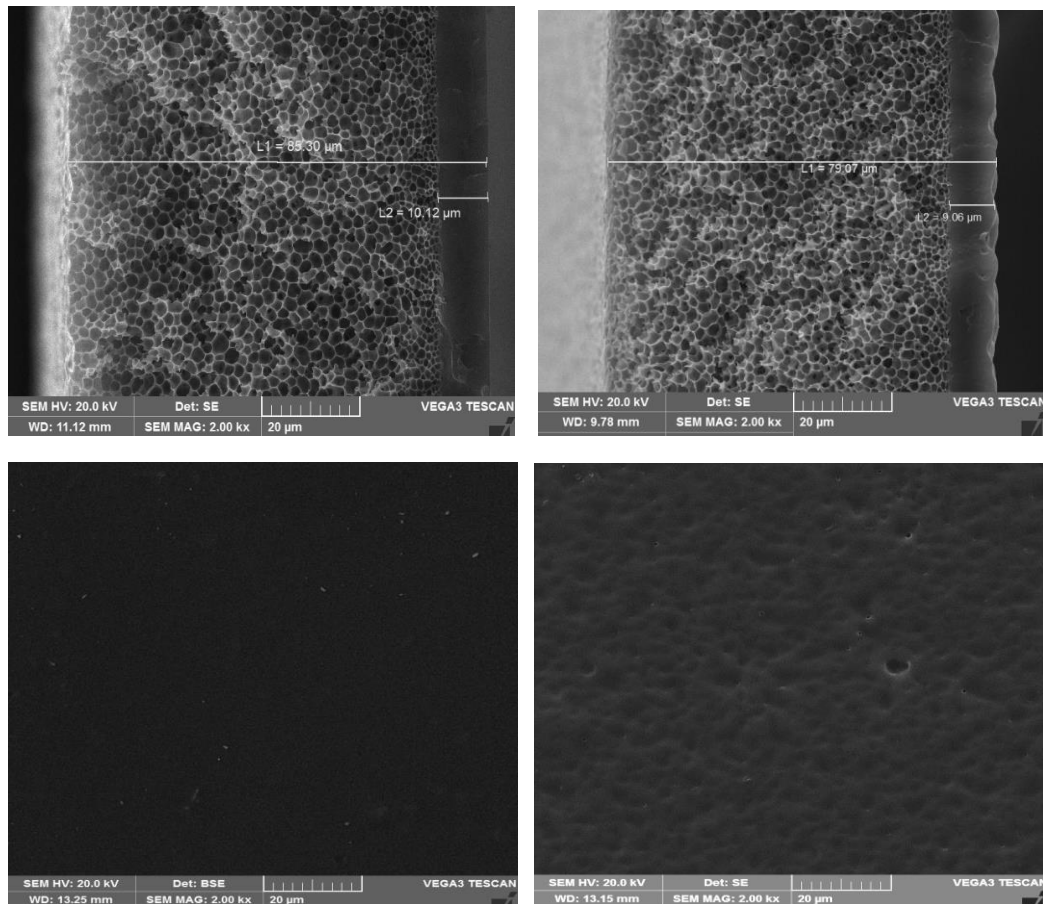
$$\alpha_{A/B} = \frac{L_A}{L_B} \quad (4.2)$$

The estimated permeability was calculated using the thickness of the dense layer.

RESULTS AND DISCUSSION

Effect of the particle content on membrane morphology

Fig 4.2 shows photomicrographs of the cross-section and the surface of the PU/PES dual layer composite membranes obtained with different AC content in the dense layer.



a)

b)

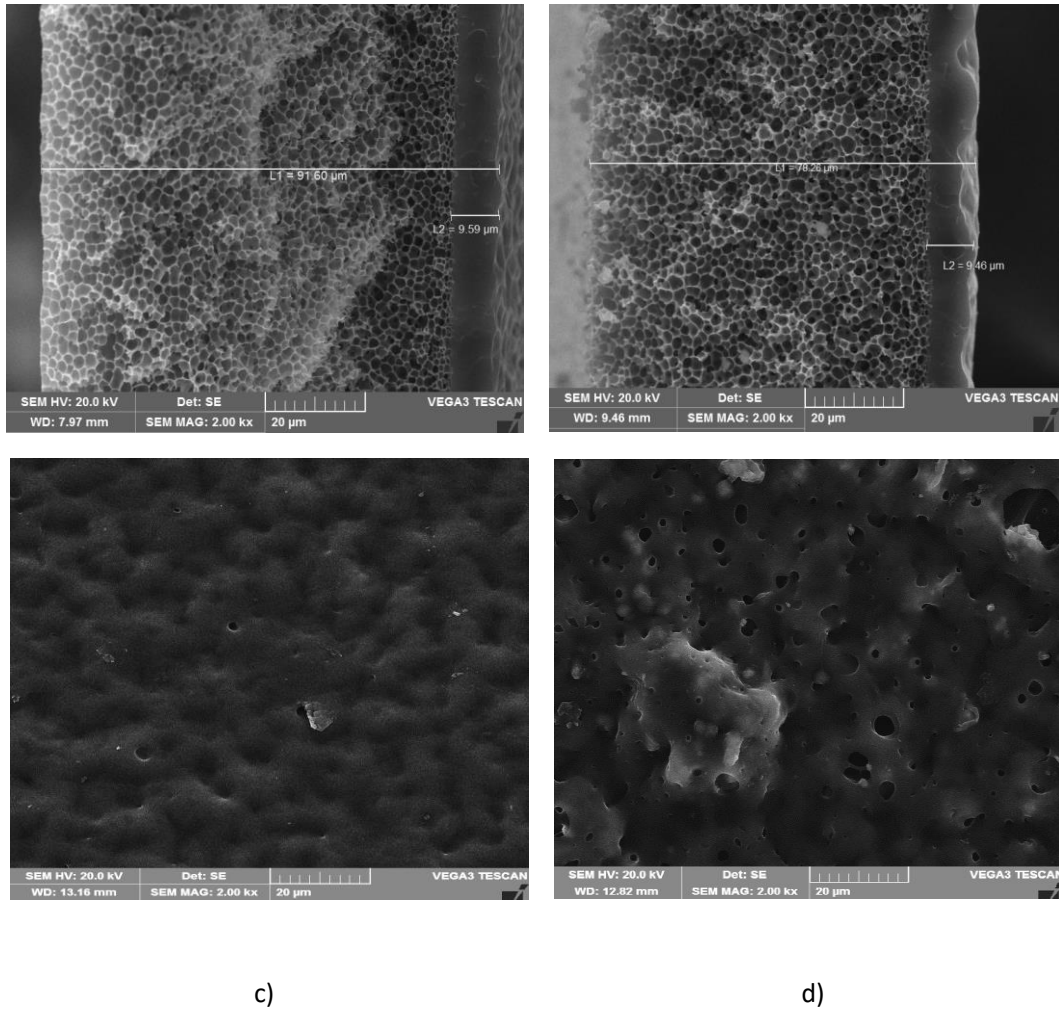
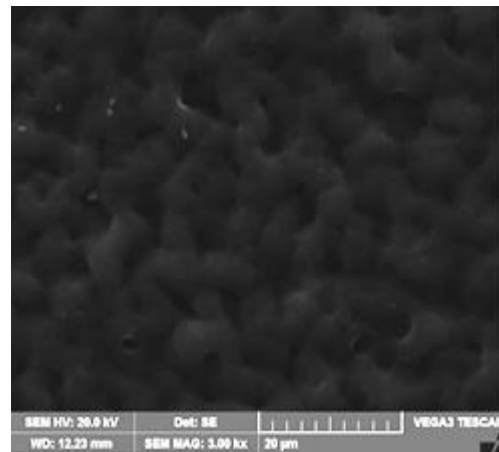
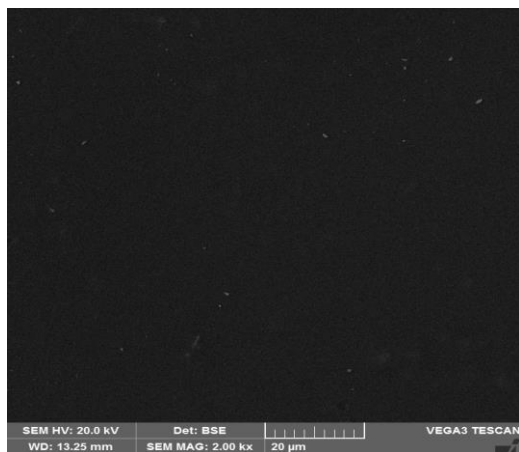
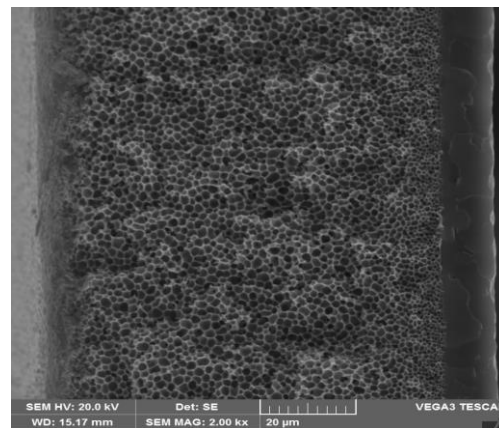
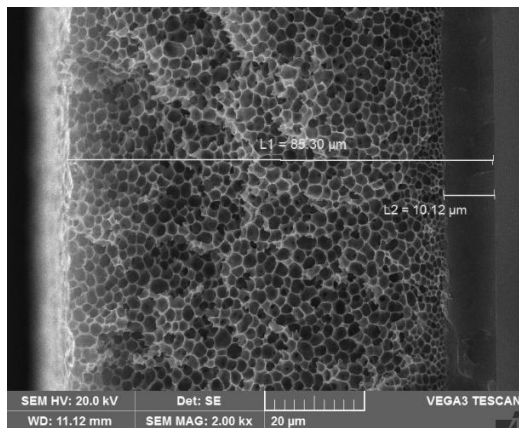


Fig 4.2. Cross-sectional and surface images of the composite membranes with different AC composition in the dense layer a) 0, b) 1, c) 2, d) 5. (AC %wt)

Increasing the AC content led to a less homogeneous surface in the dense layer, increasing the surface roughness. This could be due to THF and NMP fluxes towards water during the membrane precipitation. Thus, AC agglomeration in the surface can increase for higher AC content in the dense dope solution, which would difficult the membrane precipitation, leading to a non-homogeneous structure.

Fig 4.3 shows the PU/PES dual layer composite membranes prepared with different silica content in the dense layer.



a)

b)

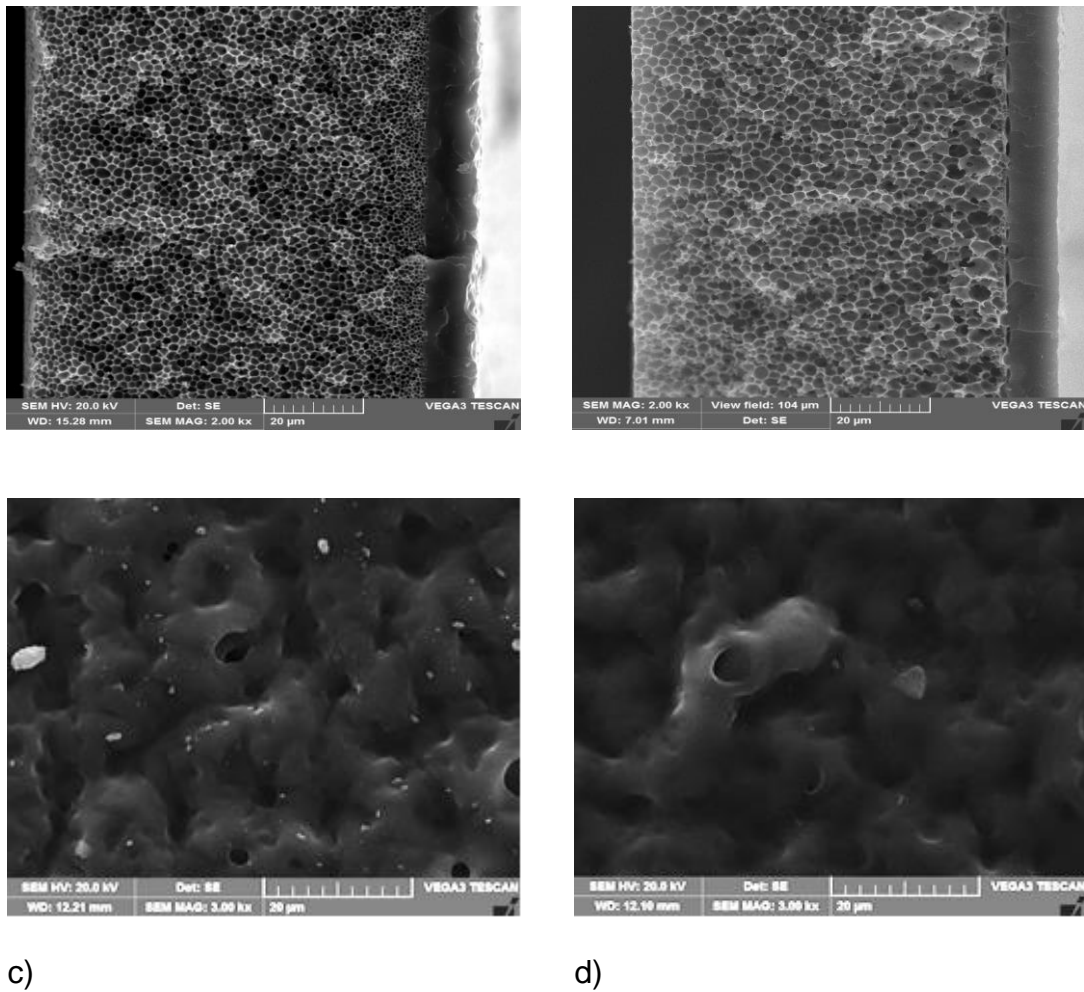


Fig 4.3. Cross-sectional and surface images of the composite membranes prepared using different silica compositions a) 0, b) 1, c) 2, d) 5. (% wt):

It can be seen that increasing the Silica content also reduced the homogeneity of the dense surface. However, at higher concentration (Fig 3d), there is a loss of adhesion between both layers. This could be the result of a higher difference between the polarity of moieties present in the particles. Activated carbon has many polar groups, such as carboxyl acids and hydroxyls, while silica particles have more non-polar groups. Polar groups may interact with the NMP solvent of the support layer favoring the adhesion phenomenon as

observed with CA particles in the selective layer. On the other hand, high content of silica particles may reduce the interaction between layers, impairing adhesion.

A SEM/EDS equipment was used in order to detect the presence of Silica in the dense layer and the Fig 4 shows the typical results for one of the membranes.

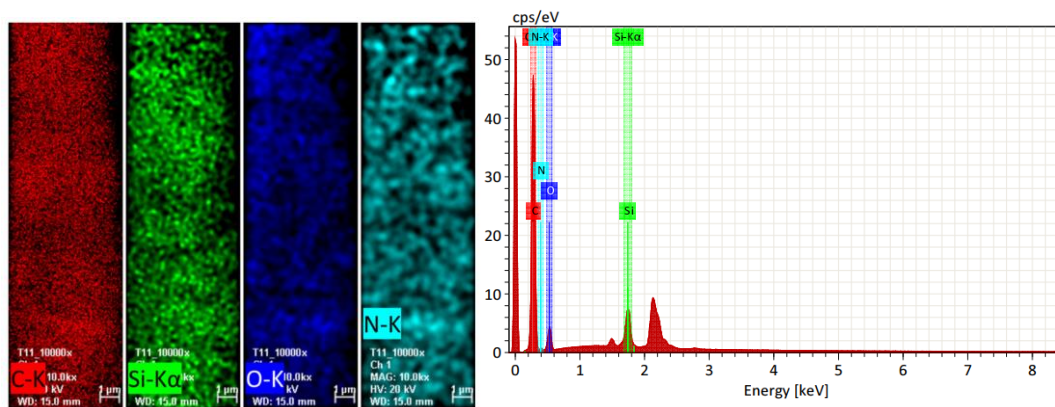


Fig 4.4. EDS images and spectrum for the dense layer with silica particles of PU/PES membranes.

According to the figure, it is possible to confirm the presence of Silica in the dense layer (green color). Moreover, the spectrum shows a peak that is representative for Si element. The technique also estimates a composition (%wt) for each element according to the size of the peak in the spectrum. In the case of silica, the values were 0.67, 1.69 and 3.65 for the M-SI1, M-SI2 and M-SI5, respectively. The expected silica content based on solution composition is shown in Table 01 and it is higher than the values obtained by SEM/EDS, suggesting some loss of particles during solution

n precipitation. It is important to stress that SEM/EDS analysis is made on a small sample and some variation of the observed values may be expected. However, in all cases the measured values were below the expected ones.

Effect of the inorganic particles on permeability and selectivity

Table 4.2 shows permeability and selectivity of pure gases for the PU/PES dual layer membranes at 1 bar and 25 °C. The dense layer thickness measured by SEM was used to calculate the gas permeabilities.

Table 4.2. PU/PES membrane permeability and selectivity at 1 bar and 25 °C.

Membrane	P_{CO_2} (Barrer)	P_{N_2} (Barrer)	P_{O_2} (Barrer)	α_{CO_2/N_2}	α_{O_2/N_2}
M-0	19.62	0.30	0.51	66.06	1.71
M-AC1	20.88	0.31	0.53	67.35	1.71
M-AC2	22.64	0.31	0.51	73.03	1.65
M-AC5	16.25	0.23	0.43	70.65	1.87
M-SI1	23.14	0.30	0.52	77.13	1.73
M-SI2	21.54	0.27	0.49	79.78	1.81
M-SI5	14.16	0.21	0.41	67.43	1.95

It can be seen that higher silica content leads to lower permeabilities, whereas an increase in activated carbon content exhibited a more complex behavior. On the other hand, the selectivities resulted in higher values when membranes are incorporated to the inorganic particles. These results are an indication that the selectivity towards CO₂ is enhanced due to a reduction in the polymer segmental mobility. This phenomenon favors the transport of more soluble molecules such as carbon dioxide. Higher values of permeabilities in membranes with AC particles may be consequence of this particle's porosity, which enhances the transport for the gases.

Effect of the feed pressure on permeability and selectivity

Table 4.3 shows permeability and selectivity for the PU/PES dual layer membranes at 25 °C for different feed pressures.

Table 4.3. Effect of pressure on permeability and selectivity of PU/PES membranes.

Membrane	Pressure (bar)	P _{CO2} (Barrer)	P _{N2} (Barrer)	P _{O2} (Barrer)	α _{CO2/N2}	α _{O2/N2}
M-0	1	19.62	0.297	0.508	66.06	1.71
	2	17.42	0.277	0.481	62.89	1.74
	4	14.77	0.245	0.461	60.29	1.88
	8	13.01	0.217	0.424	59.95	1.95
M-AC1	1	20.88	0.310	0.530	67.35	1.71
	2	18.11	0.281	0.482	64.45	1.72
	4	14.91	0.239	0.457	62.38	1.91
	8	12.87	0.208	0.411	61.88	1.98
M-AC2	1	22.64	0.31	0.51	73.03	1.65
	2	17.98	0.261	0.465	68.89	1.78
	4	13.88	0.211	0.413	65.78	1.96
	8	11.92	0.187	0.391	63.74	2.09
M-AC5	1	16.25	0.23	0.43	70.65	1.87
	2	14.14	0.211	0.409	67.01	1.94
	4	11.27	0.171	0.346	65.91	2.02
	8	9.02	0.141	0.305	63.97	2.16
M-SI1	1	23.14	0.300	0.520	77.13	1.73
	2	18.61	0.284	0.491	65.53	1.73
	4	15.16	0.241	0.457	62.90	1.90
	8	12.55	0.217	0.431	57.83	1.99
M-SI2	1	21.54	0.27	0.49	79.78	1.81
	2	17.66	0.236	0.456	74.83	1.93
	4	12.14	0.199	0.397	61.01	1.99
	8	10.01	0.163	0.363	61.41	2.23
M-SI5	1	14.16	0.21	0.41	67.43	1.95
	2	11.23	0.178	0.378	63.09	2.12
	4	9.14	0.145	0.322	63.03	2.22
	8	7.11	0.113	0.259	62.92	2.29

For all the membranes, the pressure reduced the permeability for all the gases. This result may be a consequence of the porous support mass transfer resistance, as described by the resistance-in-series model (Ullah Khan et al.,

2018a). In case of membrane with CA or Si particles, it is expected a reduction in the free volume in the polymer matrix as the pressure increases (Molki et al., 2018). In addition, since CO₂ has a higher solubility in the PU dense layer, its permeability was more affected, resulting in lower CO₂/N₂ selectivity values with pressure increase.

Figure 4.5 shows the 2008 Robeson diagram with the location of the CA and Silica dual-layer membranes (filler 2 wt%).

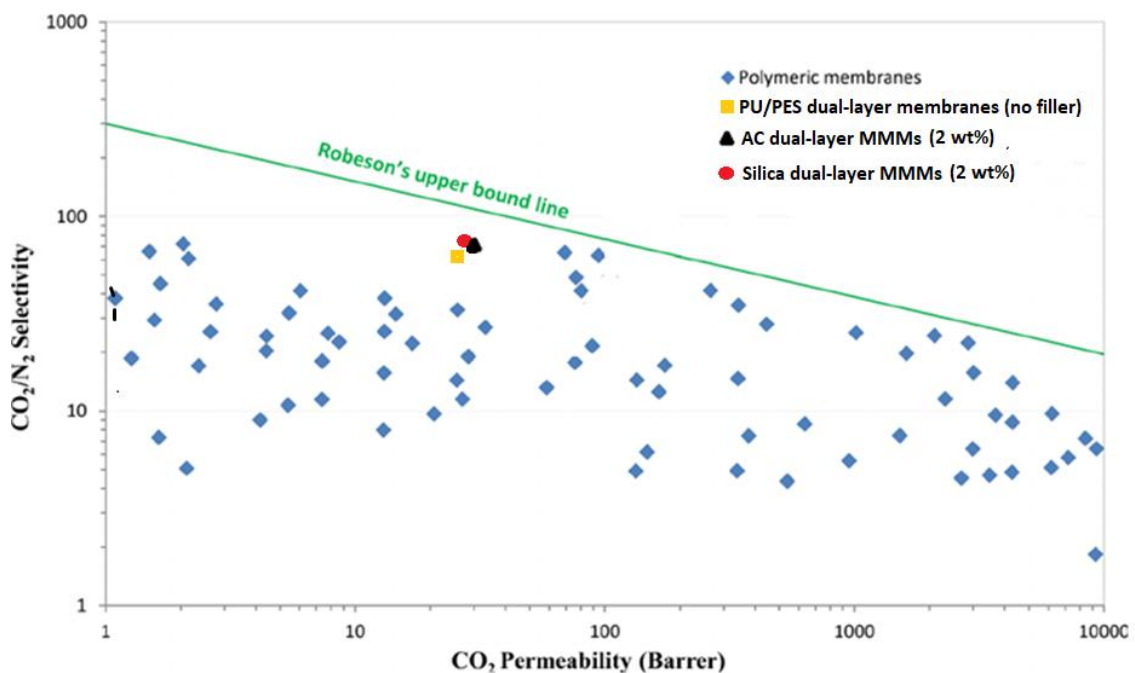
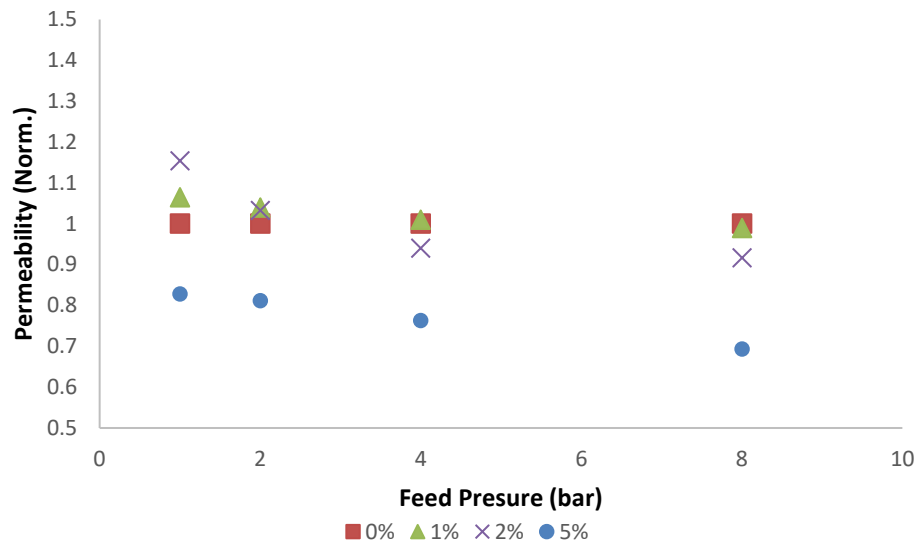


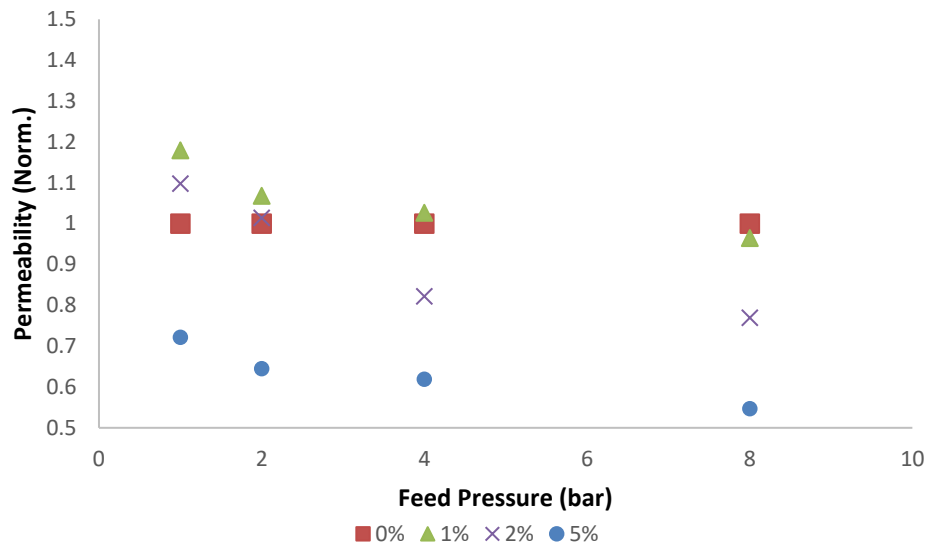
Fig 4.5. PU/PES dual-layer membranes in the 2008 Robeson diagram

It can be observed that the addition of the fillers moved the location of the membranes in the diagram closer to the upper bound line in terms of both selectivity. However, the permeability values are not still high enough compared to other membranes in the diagram. It is important to point that these fillers can be functionalized with different groups prior to the incorporation to the membrane in order to increase even more the CO₂ permeability in the membranes.

Figure 4.6 shows the normalized CO₂ permeability as function of feed pressure for membranes with different AC and Silica content, respectively. The normalized permeability is expressed taking the original PU/PES membrane permeability P₀ as a reference ($P_{norm} = P_{MMM} / P_0$).



(a)



(b)

Figure 4.6. Effect of pressure on the normalized CO₂ permeability for membranes with different inorganic particle contents (a) AC, (b) Silica.

In Figure 4.5, one may observe that the CO₂ permeability of the MMMs only exhibit significant decrease when a higher content of filler is present. This could be a result of both filler agglomeration and free volume reduction in the polymer matrix. However, the porous structure of the CA enhances the transport through the membrane, mitigating the decrease in CO₂ permeability with the filler content.

CONCLUSIONS

In this study, dual-layer MMMs were successfully prepared by the co-casting method using activated carbon and silica as fillers. According to SEM images, the adhesion and homogeneous structure was maintained for lower particle contents. However, some defects were observed in the dense surface when using higher particle content. Moreover, it was possible to confirm the presence of silica in the dense layer by SEM/EDS technique. It was found that the presence of these particles enhanced CO₂ permeability and CO₂/N₂ selectivity. Increasing the feed pressure from 1 to 8 bar led to a decrease in the permeability of all gases attributed to the porous support layer resistance. However, for higher CA particle content, it was possible to enhance more than 40% the CO₂ permeability, an effect that may be related to the transport through the porous particles, reducing the effective selective layer thickness. Furthermore, at low feed pressure the presence of the CA particles in the dense layer also enhanced CO₂/N₂ and O₂/N₂ selectivity. Those results indicated good perspective for the use of CA MMMs for flue gas treatment.

5. MAIN CONCLUSIONS AND FINAL COMMENTS

Dual-layer PU/PES membranes aiming at CO₂ removal from flue gas were successfully prepared by the co-casting method. It was possible to prepare dual-layer membranes using two different materials with similar solvent affinity. The effects of the coagulating bath temperature and solvent evaporation time were established and showed that a good layers adhesion and an homogenous support structure were obtained for a 15 s evaporation time and a water coagulating bath at 75 °C as observed by SEM.

Permeation tests in the ranges of 1-8 bar for feed pressures showed a decrease of permeability for all gases. CO₂/N₂ ideal selectivity decreased from 66 to 60 in that pressure range since CO₂ solubility into PU was more affected. On the other hand, tests performed in the range of 25-45 °C showed an enhancement of gas permeability with temperature due to a higher free-volume available in the dense layer. However, since the effect is more important for gases with higher kinetic diameter (N₂), the CO₂/N₂ selectivity decreased from 66 to 43 in that temperature range. The optimization of the co-casting method should prove useful for the fabrication of selective dual-layer membranes aimed at gas separation, allowing the use of versatile pairs of materials for the layers.

Dual-layer MMMs were successfully prepared by the co-casting method using activated carbon and silica as fillers. According to SEM images, the adhesion and homogeneous structure was maintained for lower particle contents. It was found that the presence of activated carbon and silica enhances CO₂ permeability from 19.6 to 22.6 and 23.1 Barrer, respectively. Increasing the feed pressure from 1 to 8 bar led to a decrease in the permeability of all gases

attributed to the porous support layer resistance. However, for higher CA particle content, it was possible to enhance more than 40% the CO₂ permeability, an effect that may be related to the transport through the porous particles, reducing the effective selective layer thickness. Furthermore, at low feed pressure the presence of the CA particles in the dense layer also enhanced CO₂/N₂ and O₂/N₂ selectivity. Those results indicated good perspective for the use of CA MMMs for flue gas treatment.

The main conclusions advances of the state-of-art are listed below:

- *Dual-layer polyurethane/polyethersulfone membranes were successfully prepared by the co-casting method.* From our knowledge, there are no previous works using both these polymers in a dual-layer membrane. The main reason for this is that they can be dissolved on the same kind of solvents, so it becomes difficult to maintain the stability of the layers. However, in this work, some process conditions such as evaporation time and bath temperature were evaluated in order to improve this stability.
- *Excellent adhesion and homogeneity in the layers were obtained.* There are several published articles which report the use of the co-casting technique. However, according to the SEM images, it is difficult to obtain homogeneous layers and with a good adhesion. This happens because there are several variables involved in the co-casting process including: polymers nature, layer thickness, dopes compositions, use of additives, evaporation time, and water temperature. All of these variables were taken into account in this work in order to obtain final membranes with no defects and excellent adhesion.

- *Addition of nanoparticles into the dense layer.* As it was mentioned before, the co-casting process involves several variables that must be controlled in order to obtain membranes with good structure. This control becomes more difficult when an inorganic particle is added to the process. There are some few publications that study the preparation of dual-layer mixed matrix membranes. However, there are no reports for the use of activated carbon and silica in dual-layer membranes for CO₂ capture from flue gas. Also, in this work it was possible to maintain the structure and adhesion of the layers even after including the particle in the membrane.

Suggestion for future work

Some future research directions may be pointed out, based on the results of this thesis:

- *Reduction of the dense layer thickness.* Since the highest resistance to mass transfer in the dual-layer membrane is given by the dense layer, it is recommended to reduce as much as possible the thickness of this layer. However, it is important to take into account the fluxes during the evaporation time and into the coagulation bath so the stability of the dense layer can be maintained. Also, for lower dense thickness, the stability of this layer becomes lower as well, increasing the possibility of mix of both layers prior precipitation.
- *Filler functionalization.* In order to enhance CO₂ transport through the membrane, AC and Silica fillers can be functionalized with some groups with higher affinity with CO₂ (i.e., amino groups). However, it is important

to control the particle size in order to avoid agglomeration in the membrane for higher contents.

- *Evaluation of permeation at higher temperatures.* Since the membranes were prepared for the use in CO₂ capture from flue gas, it is interesting to evaluate temperatures closer to the real situation, about 120 °C (depending on the source of the flue gas). Some of the most important factors to take into account would be: membrane stability and permeability and selectivity variation for higher temperature values.
- *Use of mixture of gases.* As it was mentioned before, it is important to test the membranes in conditions close to industrial conditions. In this work, pure gases were used for the permeation tests so all the selectivity values were ideal. It is then necessary to perform these tests using a mixture of gases.

REFERENCES

- Abanades, J. C., Arias, B., Lyngfelt, A., Mattisson, T., Wiley, D. E., Li, H., Ho, M. T., Mangano, E., & Brandani, S. (2015). Emerging CO₂ capture systems. *International Journal of Greenhouse Gas Control*, *40*, 126–166. <https://doi.org/10.1016/j.ijggc.2015.04.018>
- Afarani, H. T., Sadeghi, M., & Moheb, A. (2018). The Gas Separation Performance of Polyurethane–Zeolite Mixed Matrix Membranes. *Advances in Polymer Technology*. <https://doi.org/10.1002/adv.21672>
- Arias, A. M., Mores, P. L., Scenna, N. J., & Mussati, S. F. (2016). Optimal design and sensitivity analysis of post-combustion CO₂ capture process by chemical absorption with amines. *Journal of Cleaner Production*, *115*, 315–331. <https://doi.org/10.1016/j.jclepro.2015.12.056>
- Brunetti, A., Cersosimo, M., Sung, J., Dong, G., Fontananova, E., Moo, Y., Drioli, E., & Barbieri, G. (2017). International Journal of Greenhouse Gas Control Thermally rearranged mixed matrix membranes for CO₂ separation : An aging study. *International Journal of Greenhouse Gas Control*, *61*, 16–26. <https://doi.org/10.1016/j.ijggc.2017.03.024>
- Choi, J., Moon, D. S., Jang, J. U., Yin, W. Bin, Lee, B., & Lee, K. J. (2017). Synthesis of highly functionalized thermoplastic polyurethanes and their potential applications. *Polymer*, *116*, 287–294. <https://doi.org/10.1016/j.polymer.2017.03.083>
- Chung, T. S., Jiang, L. Y., Li, Y., & Kulprathipanja, S. (2007). Mixed matrix membranes (MMMs) comprising organic polymers with dispersed inorganic

fillers for gas separation. *Progress in Polymer Science (Oxford)*, 32(4), 483–507. <https://doi.org/10.1016/j.progpolymsci.2007.01.008>

Dai, Z., Ansaloni, L., & Deng, L. (2016). Recent advances in multi-layer composite polymeric membranes for CO₂ separation: A review. *Green Energy & Environment*, 1(2), 102–128. <https://doi.org/10.1016/j.gee.2016.08.001>

Fu, F. J., Sun, S. P., Zhang, S., & Chung, T. S. (2014). Pressure retarded osmosis dual-layer hollow fiber membranes developed by co-casting method and ammonium persulfate (APS) treatment. *Journal of Membrane Science*, 469, 488–498. <https://doi.org/10.1016/j.memsci.2014.05.063>

Garcia Jiménez, C. D., Habert, A. C., & Borges, C. P. (2021). *Polyurethane / polyethersulfone dual-layer anisotropic membranes for CO₂ removal from flue gas*. December 2020, 1–8. <https://doi.org/10.1002/app.50476>

Hashemifard, S. A., Ismail, A. F., & Matsuura, T. (2011a). Co-casting technique for fabricating dual-layer flat sheet membranes for gas separation. *Journal of Membrane Science*. <https://doi.org/10.1016/j.memsci.2011.03.053>

Hashemifard, S. A., Ismail, A. F., & Matsuura, T. (2011b). Co-casting technique for fabricating dual-layer flat sheet membranes for gas separation. *Journal of Membrane Science*, 375(1–2), 258–267. <https://doi.org/10.1016/j.memsci.2011.03.053>

Hwang, L. L., Chen, J. C., & Wey, M. Y. (2013). The properties and filtration efficiency of activated carbon polymer composite membranes for the removal of humic acid. *Desalination*, 313, 166–175.

<https://doi.org/10.1016/j.desal.2012.12.019>

Hwang, L. L., Wey, M. Y., & Chen, J. C. (2014a). Effects of membrane compositions and operating conditions on the filtration and backwashing performance of the activated carbon polymer composite membranes. *Desalination*, 352, 181–189. <https://doi.org/10.1016/j.desal.2014.08.022>

Hwang, L. L., Wey, M. Y., & Chen, J. C. (2014b). Effects of membrane compositions and operating conditions on the filtration and backwashing performance of the activated carbon polymer composite membranes. *Desalination*. <https://doi.org/10.1016/j.desal.2014.08.022>

Isfahani, A. P., Ghalei, B., Bagheri, R., Kinoshita, Y., Kitagawa, H., Sivaniah, E., & Sadeghi, M. (2016). Polyurethane gas separation membranes with etheral bonds in the hard segments. *Journal of Membrane Science*. <https://doi.org/10.1016/j.memsci.2016.04.030>

Isfahani, A. P., Sadeghi, M., Dehaghani, A. H. S., & Aravand, M. A. (2016). Enhancement of the gas separation properties of polyurethane membrane by epoxy nanoparticles. *Journal of Industrial and Engineering Chemistry*. <https://doi.org/10.1016/j.jiec.2016.08.012>

Jin Yoo, M., Hyeok Lee, J., Yeon Yoo, S., Yeon Oh, J., Min Roh, J., Grasso, G., Hyun Lee, J., Lee, D., Jin Oh, W., Yeo, J., Hoon Cho, Y., & Bum Park, H. (2018). *Defect control for large-scale thin-film composite membrane and its bench-scale demonstration*. <https://doi.org/10.1016/j.memsci.2018.09.019>

Karimi, M. B., & Hassanajili, S. (2017a). Short fiber/polyurethane composite membrane for gas separation. *Journal of Membrane Science*.

<https://doi.org/10.1016/j.memsci.2017.08.043>

Karimi, M. B., & Hassanajili, S. (2017b). Short fiber/polyurethane composite membrane for gas separation. *Journal of Membrane Science*, 543(June), 40–48. <https://doi.org/10.1016/j.memsci.2017.08.043>

Khalilpour, R., Mumford, K., Zhai, H., Abbas, A., Stevens, G., & Rubin, E. S. (2015). Membrane-based carbon capture from flue gas: A review. In *Journal of Cleaner Production*. <https://doi.org/10.1016/j.jclepro.2014.10.050>

Li, J. L., & Chen, B. H. (2005). Review of CO₂ absorption using chemical solvents in hollow fiber membrane contactors. *Separation and Purification Technology*, 41(2), 109–122. <https://doi.org/10.1016/j.seppur.2004.09.008>

Li, X. M., Ji, Y., Yin, Y., Zhang, Y. Y., Wang, Y., & He, T. (2010a). Origin of delamination/adhesion in polyetherimide/polysulfone co-cast membranes. *Journal of Membrane Science*. <https://doi.org/10.1016/j.memsci.2010.02.013>

Li, X. M., Ji, Y., Yin, Y., Zhang, Y. Y., Wang, Y., & He, T. (2010b). Origin of delamination/adhesion in polyetherimide/polysulfone co-cast membranes. *Journal of Membrane Science*, 352(1–2), 173–179. <https://doi.org/10.1016/j.memsci.2010.02.013>

Li, X. M., Ji, Y., Yin, Y., Zhang, Y. Y., Wang, Y., & He, T. (2010c). Origin of delamination/adhesion in polyetherimide/polysulfone co-cast membranes. *Journal of Membrane Science*. <https://doi.org/10.1016/j.memsci.2010.02.013>

Lillepärög, J., Breitenkamp, S., Shishatskiy, S., Pohlmann, J., Wind, J., Scholles,

- C., & Brinkmann, T. (2019). Characteristics of gas permeation behaviour in multilayer thin film composite membranes for CO₂ separation. *Membranes*, 9(2). <https://doi.org/10.3390/membranes9020022>
- Matavos-Aramyan, S., Jazebizadeh, M. H., & Babaei, S. (2020). Investigating CO₂, O₂ and N₂ permeation properties of two new types of nanocomposite membranes: Polyurethane/silica and polyesterurethane/silica. *Nano-Structures and Nano-Objects*, 21, 100414. <https://doi.org/10.1016/j.nanoso.2019.100414>
- Molki, B., Aframehr, W. M., Bagheri, R., & Salimi, J. (2018). Mixed matrix membranes of polyurethane with nickel oxide nanoparticles for CO₂ gas separation. *Journal of Membrane Science*, 549(December 2017), 588–601. <https://doi.org/10.1016/j.memsci.2017.12.056>
- Naderi, A., Chung, T. S., Weber, M., & Maletzko, C. (2019). High performance dual-layer hollow fiber membrane of sulfonated polyphenylsulfone/Polybenzimidazole for hydrogen purification. *Journal of Membrane Science*, 591(May), 117292. <https://doi.org/10.1016/j.memsci.2019.117292>
- Pereira, C. C., Nobrega, R., & Borges, C. P. (2001). Membranes obtained by simultaneous casting of two polymer solutions. *Journal of Membrane Science*. [https://doi.org/10.1016/S0376-7388\(01\)00483-5](https://doi.org/10.1016/S0376-7388(01)00483-5)
- Pierce, H. F. (1927). MEMBRANES Nitrocellulose Membranes. *Journal of Biological Chemistry*, 75(3), 795–815. [https://doi.org/10.1016/S0021-9258\(18\)84148-5](https://doi.org/10.1016/S0021-9258(18)84148-5)

- Sabetghadam, A., Liu, X., Gottmer, S., Chu, L., Gascon, J., & Kapteijn, F. (2019). Thin mixed matrix and dual layer membranes containing metal-organic framework nanosheets and Polyactive™ for CO₂ capture. *Journal of Membrane Science*, 570–571(September 2018), 226–235.
<https://doi.org/10.1016/j.memsci.2018.10.047>
- Sadeghi, M., Semsarzadeh, M. A., Barikani, M., & Ghalei, B. (2011). Study on the morphology and gas permeation property of polyurethane membranes. *Journal of Membrane Science*.
<https://doi.org/10.1016/j.memsci.2011.09.024>
- Thorbjörnsson, A., Wachtmeister, H., Wang, J., & Höök, M. (2015). Carbon capture and coal consumption: Implications of energy penalties and large scale deployment. *Energy Strategy Reviews*, 7, 18–28.
<https://doi.org/10.1016/j.esr.2014.12.001>
- Ullah Khan, I., Othman, M. H. D., Ismail, A. F., Matsuura, T., Hashim, H., Nordin, N. A. H. M., Rahman, M. A., Jaafar, J., & Jilani, A. (2018a). Status and improvement of dual-layer hollow fiber membranes via co-extrusion process for gas separation: A review. In *Journal of Natural Gas Science and Engineering*. <https://doi.org/10.1016/j.jngse.2018.01.043>
- Ullah Khan, I., Othman, M. H. D., Ismail, A. F., Matsuura, T., Hashim, H., Nordin, N. A. H. M., Rahman, M. A., Jaafar, J., & Jilani, A. (2018b). Status and improvement of dual-layer hollow fiber membranes via co-extrusion process for gas separation: A review. *Journal of Natural Gas Science and Engineering*, 52(July 2017), 215–234.
<https://doi.org/10.1016/j.jngse.2018.01.043>

- Vinoba, M., Bhagiyalakshmi, M., Alqaheem, Y., Alomair, A. A., Pérez, A., & Rana, M. S. (2017). Recent progress of fillers in mixed matrix membranes for CO₂ separation: A review. In *Separation and Purification Technology*. <https://doi.org/10.1016/j.seppur.2017.07.051>
- Wang, Meihong, Joel, A. S., Ramshaw, C., Eimer, D., & Musa, N. M. (2015). Process intensification for post-combustion CO₂ capture with chemical absorption: A critical review. *Applied Energy*, *158*, 275–291. <https://doi.org/10.1016/j.apenergy.2015.08.083>
- Wang, Ming, Wang, Z., Zhao, S., Wang, J., & Wang, S. (2017). Recent advances on mixed matrix membranes for CO₂ separation. *Chinese Journal of Chemical Engineering*, *25*(11), 1581–1597. <https://doi.org/10.1016/j.cjche.2017.07.006>
- Weigelt, F., Georgopoulos, P., Shishatskiy, S., Filiz, V., Brinkmann, T., & Abetz, V. (2018). Development and characterization of defect-free Matrimid® mixed-matrix membranes containing activated carbon particles for gas separation. *Polymers*. <https://doi.org/10.3390/polym10010051>
- Wu, D., Han, Y., Salim, W., Chen, K. K., Li, J., & Ho, W. S. W. (2018). Hydrophilic and morphological modification of nanoporous polyethersulfone substrates for composite membranes in CO₂ separation. *Journal of Membrane Science*. <https://doi.org/10.1016/j.memsci.2018.08.059>
- Xia, Q. C., Liu, M. L., Cao, X. L., Wang, Y., Xing, W., & Sun, S. P. (2018a). Structure design and applications of dual-layer polymeric membranes. *Journal of Membrane Science*, *562*(May), 85–111. <https://doi.org/10.1016/j.memsci.2018.05.033>

- Xia, Q. C., Liu, M. L., Cao, X. L., Wang, Y., Xing, W., & Sun, S. P. (2018b). Structure design and applications of dual-layer polymeric membranes. In *Journal of Membrane Science*.
<https://doi.org/10.1016/j.memsci.2018.05.033>
- Yoo, M. J., Kim, K. H., Lee, J. H., Kim, T. W., Chung, C. W., Cho, Y. H., & Park, H. B. (2018). Ultrathin Gutter Layer for High-Performance Thin-Film Composite Membranes for CO₂ Separation. *Journal of Membrane Science*, 566(June), 336–345. <https://doi.org/10.1016/j.memsci.2018.09.017>
- Zhang, Y., Sunarso, J., Liu, S., & Wang, R. (2013). Current status and development of membranes for CO₂/CH₄ separation: A review. *International Journal of Greenhouse Gas Control*, 12, 84–107.
<https://doi.org/10.1016/j.ijggc.2012.10.009>
- Zhao, S., Feron, P. H. M., Deng, L., Favre, E., Chabanon, E., Yan, S., Hou, J., Chen, V., & Qi, H. (2016). Status and progress of membrane contactors in post-combustion carbon capture: A state-of-the-art review of new developments. *Journal of Membrane Science*, 511, 180–206.
<https://doi.org/10.1016/j.memsci.2016.03.051>

ANNEX: DETAILED METHODOLOGY OF MEMBRANE SYNTHESIS AND CHARACTERIZATION

In this sections, further methodology details are given in terms of: materials, membrane preparation process, scanning electron microscopy, gas permeation measurement and variables taken into account in this thesis.

Materials

The materials, listed below, were chosen according to both preliminary tests and previous reports in literature (showed in Section 2):

- Polyurethane (PU) Ellastollan® from Basf and Tetrahydrofuran (THF) were used for the dense layer dope solution.
- Polyethersulfone (PES) ULTRASON E6020 and N-methyl-2-pyrrolidone (NMP) from Basf were used for the porous layer dope solution.
- Polyvinylpyrrolidone (PVP-K90) from Fluka was used as additive for the PES/NMP solution.
- Activated carbon (Conocco Phillips, 300 nm, porous) and Silica (Aerosil 200, Degussa-Hüls, 12 nm) were used as inorganic particles.
- CO₂, N₂ and O₂ from Linde Gases Brasil were used with purity of 99.99%.and selectivity for the PU/PES dual layer membranes at 25 °C for different feed pressures.

Membrane Preparation

This section provides specific conditions and procedures to prepare the dope solutions and the dense, dual-layer and dual-layer mixed matrix membranes.

Dope Solution

Since this process requires polymeric solutions (dope solutions) with specific composition and conditions, more details about the dope solution preparation are listed:

- Dense layer: A PU/THF (10/90 wt%) solution was prepared and stirred at 40 °C for 24h to dissolve the polymer. Then it was cooled to 25 °C.
- Dense layer for MMM: In order to avoid agglomeration, the filler was first dispersed into THF and ultra-sonicated at 60 Hz for 30 min. Then, it was mixed with the PU-THF solution (already dissolved) and stirred for 1 h to make a homogeneous solution.
- Porous layer: A PES/PVP/NMP (15/5/80 wt%) solution was prepared. First, a PES/NMP solution was first prepared and stirred at 50 °C for 24h. Then, PVP was added, stirring for additional 24h at the same temperature until total dissolution.

Dense Membranes

Dense membranes were prepared in order to compare the results with the dual-layer membranes. The process used for this preparation was:

- The solution was poured on a Teflon petri dish and dried at 25 °C for 72h.
- The obtained membrane was taken to an oven at 60 °C for 12h to remove the residual solvent.

Dual-layer membranes

Dual-layer membranes were prepared by the co-casting technique. Some conditions (i.e., cast thickness, environment temperature) were fixed according to preliminary tests and previous reported works in literature. The procedure for the dual-layer membrane preparation was:

- The support layer solution was cast on a glass plate followed by the casting of the selective layer dope solution. The cast thickness for each solution was approximately 120 μm .
- The cast dual-layer film was exposed to the environment at 25 $^{\circ}\text{C}$ to allow THF partial evaporation.
- The glass plate was then submerged for 30 min in a coagulation bath (distillated water) to induce phase separation leading to membrane formation.
- The membrane was kept in fresh water bath at room temperature for 48h to remove residual NMP, and finally dried at room temperature.

The procedure for the dual-layer MMM preparation was the same as above. The only difference was the dope solution used for the dense layer.

Filler content in the dense layer for dual-layer MMMs

For the dual-layer MMMs, activated carbon and silica were tested as fillers in the dense layer. The filler content in the membranes is given in the Table A.1.

Table A.1. Dense layer particle content in the PU/THF (10/90 wt%) dope formulation in the preparation of composite membranes. AC – Activated carbon; SI – Silica

Membrane	Particle	Content (%wt)*
M-0	none	0
M-AC1	Activated Carbon	1
M-AC2	Activated Carbon	2
M-AC5	Activated Carbon	5
M-SI1	Silica	1
M-SI2	Silica	2
M-SI5	Silica	5

*Particle content based on polymer mass

*M-0 is dual-layer membrane without filler

Scanning Electron Microscopy (SEM)

Scanning Electron Microscopy (SEM) Vega (Tescan 3) was used to characterize the morphology and thickness of the dense and dual-layer membranes. Moreover, Scanning Electron Microscopy integrated with Energy Dispersive X-Ray Spectroscopy (SEM/EDS) Vega (Tescan 3) was used to investigate the silica distribution through the membrane and to estimate its composition in the dense layer. The thickness of each layer in the composite membrane was an average value taken from ten different locations in the samples.

Gas permeation measurement

Figure A.1. shows the system used in this work for gas permeation.

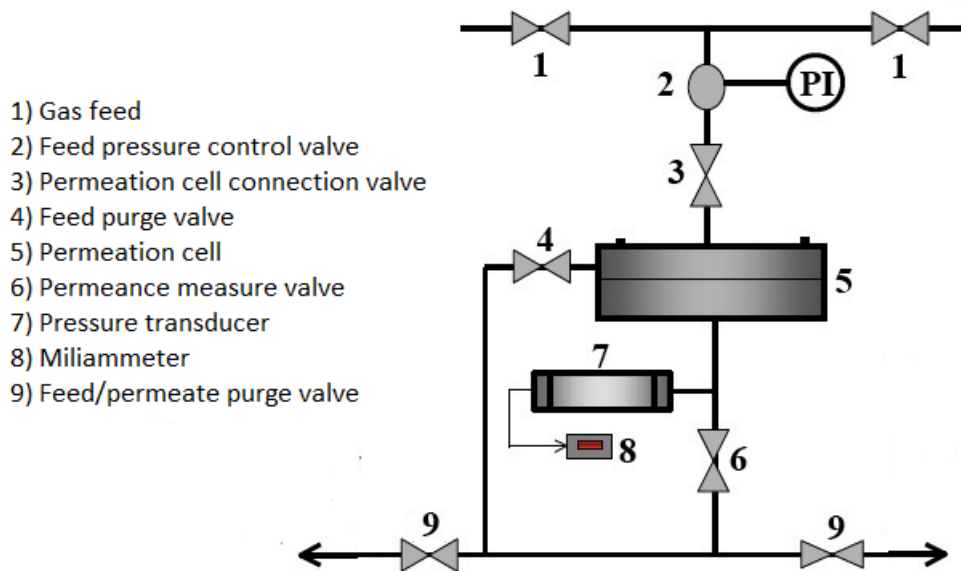


Figure A.1. Diagram of the permeation system for pure gases

The permeance in the membrane is calculated based on the variation of the pressure measured by the transducer during the test time. The specific conditions and details for this process were:

- Membranes that showed better morphology were tested in gas permeation for pure CO₂, N₂ and O₂.
- Each sample was sealed into a circular cell with an effective area of 8.5 cm².
- The permeance L in GPU was calculated using:

$$L = \left(\frac{T_{STP}}{T P_{STP}} \right) \left(\frac{V_d}{A \Delta P} \right) \left(\frac{dP}{dt} \right)_{SS}$$

- The ideal selectivity $\alpha_{A/B}$ was calculated by using:

$$\alpha_{A/B} = \frac{L_A}{L_B}$$

- And estimated permeability value was calculated by using only the thickness of the dense layer:

$$P_i = L_i * \delta_{dl}$$

Variables for this thesis

According to preliminary tests and previous works reported in literature, some variables and values were chosen to be studied in this thesis.

Dual-layer membrane preparation:

- Coagulation bath temperature: 25, 50 and 75 °C.
- Exposure time (prior to immersion in coagulation bath): 5, 15, 30 s.

Gas permeation with dual-layer membranes:

- Feed pressure: 1, 2, 4 and 8 bar.
- Temperature: 25, 35 and 45 °C.

Dual-layer mixed matrix membrane preparation:

- Filler nature: Activated Carbon and Silica.
- Filler content in the dense layer: 1, 2 and 5 wt%.

Gas permeation with dual-layer mixed matrix membranes:

- Feed pressure: 1, 2, 4 and 8 bar.